Available online at www.sciencedirect.com
ScienceDirect
ELSEVIER
Journal of Computational and Applied Mathematics 200 (2007) 653 – 676
JOURNAL OF COMPUTATIONAL AND APPLIED MATHEMATICS
www.elsevier.com/locate/cam

An augmented mixed finite element method with Lagrange multipliers: A priori and a posteriori error analyses ☆

Tomás P. Barrios[a], Gabriel N. Gatica[b,*]

[a] *Facultad de Ingeniería, Universidad Católica de la Santísima Concepción, Casilla 297, Concepción, Chile*
[b] *GI²MA, Departamento de Ingeniería Matemática, Universidad de Concepción, Casilla 160-C, Concepción, Chile*

Received 27 August 2005; received in revised form 9 January 2006

Abstract

In this paper, we provide a priori and a posteriori error analyses of an augmented mixed finite element method with Lagrange multipliers applied to elliptic equations in divergence form with mixed boundary conditions. The augmented scheme is obtained by including the Galerkin least-squares terms arising from the constitutive and equilibrium equations. We use the classical Babuška–Brezzi theory to show that the resulting dual-mixed variational formulation and its Galerkin scheme defined with Raviart–Thomas spaces are well posed, and also to derive the corresponding a priori error estimates and rates of convergence. Then, we develop a reliable and efficient residual-based a posteriori error estimate and a reliable and quasi-efficient Ritz projection-based one, as well. Finally, several numerical results illustrating the performance of the augmented scheme and the associated adaptive algorithms are reported.

Keywords: Mixed finite elements; Raviart–Thomas spaces; A posteriori error estimates

1. Introduction

In the recent paper [2], a modified mixed finite element method solving second order elliptic equations in divergence form with mixed boundary conditions is introduced and analyzed. The approach there imposes the essential (Neumann) boundary condition in a weak sense, which yields the introduction of a further Lagrange multiplier given precisely by the trace of the solution on the Neumann boundary. Indeed, as it is well known, the possibility of introducing auxiliary unknowns of physical interest, such as traces, fluxes, stresses, and others, constitutes one of the main advantages of applying dual-mixed variational formulations to solve diverse problems in continuum mechanics. These additional unknowns can then be approximated directly, thus avoiding the numerical postprocessing that is usually employed with the solutions arising from primal formulations. Consequently, the derivation of appropriate finite element subspaces yielding well-posed Galerkin schemes and a priori error estimates has been extensively studied and several choices are already available for a large class of linear and even nonlinear boundary value problems (see, e.g. [3,5,8,20,22],

☆ This research was partially supported by CONICYT-Chile through the FONDAP Program in Applied Mathematics, and by the Dirección de Investigación of the Universidad de Concepción through the Advanced Research Groups Program.
* Corresponding author.
E-mail addresses: tomas@ucsc.cl (T.P. Barrios), ggatica@ing-mat.udec.cl (G.N. Gatica).

0377-0427/$ - see front matter © 2006 Elsevier B.V. All rights reserved.
doi:10.1016/j.cam.2006.01.017

and the references therein). The key issue of this analysis is certainly the verification of the discrete inf–sup conditions involved. The corresponding a posteriori error analysis of the method from [2] was provided in [19]. The results in [19] include a reliable and efficient estimate based on residuals, and a reliable and quasi-efficient Bank–Weiser type estimate based on local problems.

On the other hand, an alternative approach that has also been widely investigated is the stabilization of dual-mixed variational formulations through the application of diverse techniques. A quite general procedure to this respect is given by the Galerkin least-squares methods, also known as augmented variational formulations, which go back to [14,15]. These methods are certainly not restricted to dual-mixed schemes, and have already been extended in different directions. In particular, some applications to elasticity problems can be found in [16,7], a non-symmetric variant was considered in [13] for the Stokes problem, and a stabilized mixed finite element method for Darcy flow was recently introduced in [21]. An abstract framework concerning the stabilization of general mixed finite element methods can be seen in [6].

Consequently, the main purpose of this paper is to employ suitable Galerkin least-squares terms to augment the mixed finite element method from [2] and then derive the associated a priori and a posteriori error analyses of the resulting variational formulation. We remark that this augmented scheme allows us to approximate simultaneously the main unknown, the flux, and the Neumann trace, with Galerkin solutions in finite element subspaces of $H^1_{\Gamma_\mathrm{D}}(\Omega)$, $H(\mathrm{div};\Omega)$, and $H^{1/2}_{00}(\Gamma_\mathrm{N})$, respectively, where Ω is the domain under consideration, Γ_N (resp Γ_D) is the Neumann (resp. Dirichlet) boundary, $H^1_{\Gamma_\mathrm{D}}(\Omega) := \{v \in H^1(\Omega) : v = 0 \text{ on } \Gamma_\mathrm{D}\}$, and $H^{1/2}_{00}(\Gamma_\mathrm{N}) := \{v|_{\Gamma_\mathrm{N}} : \ v \in H^1_{\Gamma_\mathrm{D}}(\Omega)\}$. In particular, the present approach works for any subspace of $H^1_{\Gamma_\mathrm{D}}(\Omega)$, which differs from the mixed method in [2,19] where the inf–sup conditions needed for the stability of the corresponding Galerkin scheme only hold for some subspaces of $L^2(\Omega)$ approximating the main unknown. The rest of our work is organized as follows. In Section 2, we introduce the model boundary value problem, define the augmented variational formulation, and show that it is well posed. In Section 3, we define the augmented mixed finite element scheme, prove its stability, and establish the corresponding a priori error estimate. In Section 4, we deduce a reliable and efficient residual-based a posteriori error estimate. Edge and triangle bubble functions are employed there to show the corresponding efficiency. Next, a reliable and quasi-efficient Ritz projection-based a posteriori error estimate is introduced and analyzed in Section 5. Finally, in Section 6, we present several numerical examples illustrating the performance of the augmented scheme and the associated adaptive algorithms.

Throughout this paper, c and C, with or without subscripts, bars, tildes or hats, denote positive constants, independent of the parameters and functions involved, which may take different values at different occurrences.

2. The augmented mixed variational formulation

Let Ω be a simply connected domain in $\mathbb{R}^2$ with polygonal boundary Γ, and such that all its interior angles lie in $(0, 2\pi)$. Further, let Γ_D and Γ_N be disjoint open subsets of Γ, with $|\Gamma_\mathrm{D}|, |\Gamma_\mathrm{N}| \neq 0$, such that $\Gamma = \bar{\Gamma}_\mathrm{D} \cup \bar{\Gamma}_\mathrm{N}$. Then, given $f \in L^2(\Omega)$ and $g \in H^{-1/2}(\Gamma_\mathrm{N})$, we consider the model boundary value problem: find $u \in H^1(\Omega)$ such that

$$-\Delta u = f \quad \text{in } \Omega, \quad u = 0 \quad \text{on } \Gamma_\mathrm{D}, \quad \frac{\partial u}{\partial \boldsymbol{v}} = g \quad \text{on } \Gamma_\mathrm{N}, \tag{2.1}$$

where $\boldsymbol{v}$ is the unit outward normal vector to Γ. We recall that the Sobolev space $H^{-1/2}(\Gamma_\mathrm{N})$ is the dual of $H^{1/2}_{00}(\Gamma_\mathrm{N})$ (already defined above in Section 1). The corresponding duality pairing with respect to the $L^2(\Gamma_\mathrm{N})$—inner product is denoted by $\langle\cdot,\cdot\rangle_{\Gamma_\mathrm{N}}$.

Since we are interested in applying mixed finite element methods to solve (2.1), we define the auxiliary unknowns $\boldsymbol{\sigma} := \nabla u$ in Ω and $\xi = -u$ on Γ_N. Hence, proceeding in the usual way (see [2] for details), we arrive to the following mixed variational formulation of (2.1): find $((\boldsymbol{\sigma}, u), \xi) \in H \times Q$ such that

$$\begin{aligned} &a((\boldsymbol{\sigma}, u), (\boldsymbol{\tau}, v)) + b((\boldsymbol{\tau}, v), \xi) = \int_\Omega f v \quad \forall (\boldsymbol{\tau}, v) \in H, \\ &b((\boldsymbol{\sigma}, u), \lambda) = \langle g, \lambda \rangle_{\Gamma_\mathrm{N}} \quad \forall \lambda \in Q, \end{aligned} \tag{2.2}$$

where $H := H(\mathrm{div};\Omega) \times L^2(\Omega)$, $Q := H_{00}^{1/2}(\Gamma_{\mathrm{N}})$, and the bilinear forms $a : H \times H \to \mathbb{R}$ and $b : H \times Q \to \mathbb{R}$ are given by

$$a((\boldsymbol{\zeta}, w), (\boldsymbol{\tau}, v)) := \int_\Omega \boldsymbol{\zeta} \cdot \boldsymbol{\tau} + \int_\Omega w \operatorname{div} \boldsymbol{\tau} - \int_\Omega v \operatorname{div} \boldsymbol{\zeta},$$

$$b((\boldsymbol{\tau}, v), \lambda) := \langle \boldsymbol{\tau} \cdot \boldsymbol{v}, \lambda \rangle_{\Gamma_{\mathrm{N}}},$$

for all $(\boldsymbol{\zeta}, w), (\boldsymbol{\tau}, v) \in H$ and for all $\lambda \in Q$. The well posedness of (2.2) is established by Theorem 2.1 in [2].

Now, it is not difficult to see that u really lives in the space $H^1_{\Gamma_{\mathrm{D}}}(\Omega)$. Hence, we now proceed as in [4,18,21], and include the Galerkin least-squares terms given by

$$\frac{1}{2} \int_\Omega (\nabla u - \boldsymbol{\sigma}) \cdot (\nabla v + \boldsymbol{\tau}) = 0 \quad \forall (\boldsymbol{\tau}, v) \in H(\mathrm{div};\Omega) \times H^1_{\Gamma_{\mathrm{D}}}(\Omega) \tag{2.3}$$

and

$$\int_\Omega \operatorname{div} \boldsymbol{\sigma} \operatorname{div} \boldsymbol{\tau} = - \int_\Omega f \operatorname{div} \boldsymbol{\tau} \quad \forall \boldsymbol{\tau} \in H(\mathrm{div};\Omega). \tag{2.4}$$

Thus, adding the Eqs. (2.2)–(2.4), we obtain the following augmented mixed variational formulation: find $((\boldsymbol{\sigma}, u), \xi) \in \mathbf{H} \times Q$ such that

$$\begin{aligned} &A((\boldsymbol{\sigma}, u), (\boldsymbol{\tau}, v)) + B((\boldsymbol{\tau}, v), \xi) = F(\boldsymbol{\tau}, v) \quad \forall (\boldsymbol{\tau}, v) \in \mathbf{H}, \\ &B((\boldsymbol{\sigma}, u), \lambda) = G(\lambda) \quad \forall \lambda \in Q, \end{aligned} \tag{2.5}$$

where $\mathbf{H} := H(\mathrm{div};\Omega) \times H^1_{\Gamma_{\mathrm{D}}}(\Omega)$, and the bilinear forms $A : \mathbf{H} \times \mathbf{H} \to \mathbb{R}$ and $B : \mathbf{H} \times Q \to \mathbb{R}$, and the linear functionals $F : \mathbf{H} \to \mathbb{R}$ and $G : Q \to \mathbb{R}$, are given by

$$\begin{aligned} A((\boldsymbol{\zeta}, w), (\boldsymbol{\tau}, v)) := &\int_\Omega \boldsymbol{\zeta} \cdot \boldsymbol{\tau} + \int_\Omega w \operatorname{div} \boldsymbol{\tau} - \int_\Omega v \operatorname{div} \boldsymbol{\zeta} \\ &+ \int_\Omega \operatorname{div}(\boldsymbol{\zeta}) \operatorname{div}(\boldsymbol{\tau}) + \frac{1}{2} \int_\Omega (\nabla w - \boldsymbol{\zeta}) \cdot (\nabla v + \boldsymbol{\tau}), \end{aligned} \tag{2.6}$$

$$B((\boldsymbol{\tau}, v), \lambda) := \langle \boldsymbol{\tau} \cdot \boldsymbol{v}, \lambda \rangle_{\Gamma_{\mathrm{N}}}, \tag{2.7}$$

$$F(\boldsymbol{\tau}, v) := \int_\Omega f v - \int_\Omega f \operatorname{div} \boldsymbol{\tau}, \tag{2.8}$$

and

$$G(\lambda) := \langle g, \lambda \rangle_{\Gamma_{\mathrm{N}}}, \tag{2.9}$$

for all $(\boldsymbol{\zeta}, w), (\boldsymbol{\tau}, v) \in \mathbf{H}$ and for all $\lambda \in Q$.

We remark here that the inclusion of the factor $\frac{1}{2}$ in the definition of A will become clear from the proof of Theorem 2.1. Actually, it could be taken as any number in $(0, 1)$. In addition, we notice that the augmented formulation (2.5) is still written in a dual-mixed structure. In fact, in order to apply below some results from [2], we need the term dealing with the Neumman boundary condition to be kept separate (in the form of B). This approach differs from the one in [4] where the dual-mixed setting is avoided by introducing an additional boundary residual term expressed in the $H^{1/2}$ Sobolev norm by means of wavelet bases.

Now, since the seminorm $|\cdot|_{H^1(\Omega)}$ and the norm $\|\cdot\|_{H^1(\Omega)}$ of the Sobolev space $H^1(\Omega)$ are equivalent in $H^1_{\Gamma_{\mathrm{D}}}(\Omega)$, we can define

$$\|(\boldsymbol{\tau}, v)\|^2_{\mathbf{H}} := \|\boldsymbol{\tau}\|^2_{H(\mathrm{div};\Omega)} + |v|^2_{H^1(\Omega)} \quad \forall (\boldsymbol{\tau}, v) \in \mathbf{H}.$$

Hence, A, B, F and G are all bounded with constants $\|A\|$, $\|B\|$, $\|F\|$, and $\|G\|$, respectively.

The following result establishes that (2.5) is well posed.

Theorem 2.1. *There exists a unique* $((\boldsymbol{\sigma}, u), \xi) \in \mathbf{H} \times Q$ *solution of the variational problem* (2.5) *and the following continuous dependence result holds*:

$$\|((\boldsymbol{\sigma}, u), \xi)\|_{\mathbf{H}\times Q} \leqslant C\{\|F\|_{\mathbf{H}'} + \|G\|_{Q'}\} \leqslant C\{\|f\|_{L^2(\Omega)} + \|g\|_{H^{-1/2}(\Gamma_{\rm N})}\}. \tag{2.10}$$

Proof. We first recall from Theorem 2.1 in [2] that the bilinear form B satisfies the continuous inf–sup condition. More precisely, there exists $C > 0$ such that

$$\sup_{\substack{(\boldsymbol{\tau},v)\in\mathbf{H}\\(\boldsymbol{\tau},v)\neq 0}} \frac{B((\boldsymbol{\tau}, v), \lambda)}{\|(\boldsymbol{\tau}, v)\|_{\mathbf{H}}} \geqslant \sup_{\substack{\boldsymbol{\tau}\in H(\mathrm{div};\Omega)\\ \mathrm{div}\,\boldsymbol{\tau}=0,\boldsymbol{\tau}\neq 0}} \frac{B((\boldsymbol{\tau}, 0), \lambda)}{\|\boldsymbol{\tau}\|_{H(\mathrm{div};\Omega)}} = \sup_{\substack{\boldsymbol{\tau}\in H(\mathrm{div};\Omega)\\ \mathrm{div}\,\boldsymbol{\tau}=0,\boldsymbol{\tau}\neq 0}} \frac{\langle \boldsymbol{\tau}\cdot\boldsymbol{v}, \lambda\rangle_{\Gamma_{\rm N}}}{\|\boldsymbol{\tau}\|_{H(\mathrm{div};\Omega)}} \geqslant C\|\lambda\|_{H^{1/2}_{00}(\Gamma_{\rm N})} \tag{2.11}$$

for all $\lambda \in Q$. Also, we easily find from the definition of A in (2.6) that

$$A((\boldsymbol{\tau}, v), (\boldsymbol{\tau}, v)) = \tfrac{1}{2}\|\boldsymbol{\tau}\|^2_{[L^2(\Omega)]^2} + \|\mathrm{div}\,\boldsymbol{\tau}\|^2_{L^2(\Omega)} + \tfrac{1}{2}|v|^2_{H^1(\Omega)} \geqslant \tfrac{1}{2}\|(\boldsymbol{\tau}, v)\|^2_{\mathbf{H}} \tag{2.12}$$

for all $(\boldsymbol{\tau}, v) \in \mathbf{H}$, and hence, in particular, A is strongly coercive on the kernel of the operator associated to B. The rest of the proof is a simple application of the classical Babuška–Brezzi theory (see, e.g., [5, Theorem 1.1, Chapter II]). □

3. The augmented Galerkin scheme

Let $\{\mathscr{T}_h\}_{h>0}$ be a regular family of triangulations of $\bar{\Omega}$ made of straight side triangles T of diameter h_T such that $h := \max\{h_T : T \in \mathscr{T}_h\}$. We assume that all the points in $\bar{\Gamma}_{\rm D} \cap \bar{\Gamma}_{\rm N}$ become vertices of $\mathscr{T}_h$ for all $h > 0$. Then, the finite element subspace M_h for the unknown $\boldsymbol{\sigma} \in H(\mathrm{div}; \Omega)$ is defined as the Raviart–Thomas space of order zero, that is

$$M_h := \{\boldsymbol{\tau}_h \in H(\mathrm{div}; \Omega) : \boldsymbol{\tau}_h|_T \in \mathrm{RT}_0(T)\ \forall T \in \mathscr{T}_h\}, \tag{3.1}$$

where $\mathrm{RT}_0(T) := \mathrm{span}\left\{\begin{pmatrix}1\\0\end{pmatrix}, \begin{pmatrix}0\\1\end{pmatrix}, \begin{pmatrix}x_1\\x_2\end{pmatrix}\right\}$ for each $T \in \mathscr{T}_h$, and $x := \begin{pmatrix}x_1\\x_2\end{pmatrix}$ represents a generic vector of $\mathbb{R}^2$.

Next, we let $\{\Gamma_1, \Gamma_2, \ldots, \Gamma_n\}$ be the partition on $\Gamma_{\rm N}$ induced by the triangulation $\mathscr{T}_h$, and assume that $\{\mathscr{T}_h\}_{h>0}$ is uniformly regular near $\Gamma_{\rm N}$, that is there exists $C > 0$, independent of h, such that $|\Gamma_j| \geqslant Ch$ for all $j \in \{1, \ldots, n\}$, for all $h > 0$. In addition, we introduce an independent partition $\{\tilde{\Gamma}_1, \tilde{\Gamma}_2, \ldots, \tilde{\Gamma}_m\}$ of $\Gamma_{\rm N}$, denote $\tilde{h} := \max\{|\tilde{\Gamma}_j| : j \in \{1, \ldots, m\}\}$, and assume that this partition is also uniformly regular, which means that there exists $C > 0$ such that $|\tilde{\Gamma}_j| \geqslant C\tilde{h}$ for all $j \in \{1, \ldots, m\}$, for all $\tilde{h} > 0$. Then, we define the finite element subspace $Q_{\tilde{h}}$ for the unknown $\xi \in H^{1/2}_{00}(\Gamma_{\rm N})$ as

$$Q_{\tilde{h}} := \{\lambda_{\tilde{h}} \in H^{1/2}_{00}(\Gamma_{\rm N}) : \quad \lambda_{\tilde{h}}|_{\tilde{\Gamma}_j} \in \mathbf{P}_1(\tilde{\Gamma}_j) \quad \forall j \in \{1, \ldots, m\}\}. \tag{3.2}$$

Hereafter, given a non-negative integer k and a subset S of $\mathbb{R}^2$, $\mathbf{P}_k(S)$ stands for the space of polynomials defined on S of degree $\leqslant k$.

Lemma 3.1. *There exist* $C_0, \beta^* > 0$, *independent of* h *and* $\tilde{h}$, *such that for all* $h \leqslant C_0\tilde{h}$ *there holds*

$$\sup_{\substack{\boldsymbol{\tau}_h\in M_h\\ \boldsymbol{\tau}_h\neq 0}} \frac{B((\boldsymbol{\tau}_h, 0), \lambda_{\tilde{h}})}{\|\boldsymbol{\tau}_h\|_{H(\mathrm{div};\Omega)}} = \sup_{\substack{\boldsymbol{\tau}_h\in M_h\\ \boldsymbol{\tau}_h\neq 0}} \frac{\langle \boldsymbol{\tau}_h\cdot\boldsymbol{v}, \lambda_{\tilde{h}}\rangle_{\Gamma_{\rm N}}}{\|\boldsymbol{\tau}_h\|_{H(\mathrm{div};\Omega)}} \geqslant \beta^*\|\lambda_{\tilde{h}}\|_{H^{1/2}_{00}(\Gamma_{\rm N})} \quad \forall \lambda_{\tilde{h}} \in Q_{\tilde{h}}. \tag{3.3}$$

Proof. It follows from Lemmata 3.2 and 3.3 in [2], which make use of the above assumptions on the partitions of $\Gamma_{\rm N}$. □

We now let X_h be any finite element subspace for the unknown $u \in H^1_{\Gamma_{\rm D}}(\Omega)$. In particular, we may consider the continuous piecewise linear functions, that is

$$X_h := \{v_h \in H^1_{\Gamma_{\rm D}}(\Omega) : v_h|_T \in \mathbf{P}_1(T)\ \forall T \in \mathscr{T}_h\}. \tag{3.4}$$

Hence, denoting $\mathbf{H}_h := M_h \times X_h$, the mixed finite element scheme associated to the augmented formulation (2.5) reads as follows: Find $((\boldsymbol{\sigma}_h, u_h), \xi_{\tilde{h}}) \in \mathbf{H}_h \times Q_{\tilde{h}}$ such that

$$A((\boldsymbol{\sigma}_h, u_h), (\boldsymbol{\tau}_h, v_h)) + B((\boldsymbol{\tau}_h, v_h), \xi_{\tilde{h}}) = F(\boldsymbol{\tau}_h, v_h) \quad \forall (\boldsymbol{\tau}_h, v_h) \in \mathbf{H}_h,$$
$$B((\boldsymbol{\sigma}_h, u_h), \lambda_{\tilde{h}}) = G(\lambda_{\tilde{h}}) \quad \forall \lambda_{\tilde{h}} \in Q_{\tilde{h}}. \tag{3.5}$$

The following theorem establishes the unique solvability, stability, and convergence of (3.5).

Theorem 3.1. *For each $h \leqslant C_0 \tilde{h}$ the mixed finite element scheme* (3.5) *has a unique solution* $((\boldsymbol{\sigma}_h, u_h), \xi_{\tilde{h}}) \in \mathbf{H}_h \times Q_{\tilde{h}}$. *Moreover, there exist* $C_1, C_2 > 0$, *independent of h and $\tilde{h}$, such that*

$$\|((\boldsymbol{\sigma}_h, u_h), \xi_{\tilde{h}})\|_{\mathbf{H}\times Q} \leqslant C_1 \{\|f\|_{L^2(\Omega)} + \|g\|_{H^{-1/2}(\Gamma)}\},$$

and

$$\|((\boldsymbol{\sigma}, u), \xi) - ((\boldsymbol{\sigma}_h, u_h), \xi_{\tilde{h}})\|_{\mathbf{H}\times Q} \leqslant C_2 \inf_{((\boldsymbol{\tau}_h, v_h), \lambda_{\tilde{h}}) \in \mathbf{H}_h \times Q_{\tilde{h}}} \|((\boldsymbol{\sigma}, u), \xi) - ((\boldsymbol{\tau}_h, v_h), \lambda_{\tilde{h}})\|_{\mathbf{H}\times Q}.$$

Proof. The discrete inf–sup condition for B is provided by Lemma 3.1, independently of the choice of X_h, whereas the strong coerciveness of A on the discrete kernel of B, which is a subspace of $\mathbf{H}_h$ and hence of $\mathbf{H}$, is trivially guaranteed by (2.12). Therefore, a straightforward application of the abstract Theorems 1.1 and 2.1 in Chapter II of [5] completes the proof. □

Because of the condition $h \leqslant C_0 \tilde{h}$, we assume from now on, without loss of generality, that each edge Γ_i is contained in an edge $\tilde{\Gamma}_j$, for some $j \in \{1, \ldots, m\}$. Certainly, this requires implicitly that the end points of $\tilde{\Gamma}_j$ be vertices of $\mathscr{T}_h$, which is also assumed in what follows. This section is completed with a result on the rate of convergence of the mixed finite element (3.5).

Theorem 3.2. *Let* $((\boldsymbol{\sigma}, u), \xi)$ *and* $((\boldsymbol{\sigma}_h, u_h), \xi_{\tilde{h}})$ *be the unique solutions of the continuous and discrete mixed formulations* (2.5) *and* (3.5), *respectively. Assume that* $\boldsymbol{\sigma} \in [H^r(\Omega)]^2$, $\operatorname{div} \boldsymbol{\sigma} \in H^r(\Omega)$, $u \in H^{r+1}(\Omega)$, *and* $\xi \in H^{r+1/2}(\Gamma_{\mathrm{N}})$ *for some* $r \in (0, 1]$. *Then, there exists* $C > 0$, *independent of h and $\tilde{h}$, such that*

$$\begin{aligned} &\|((\boldsymbol{\sigma}, u), \xi) - ((\boldsymbol{\sigma}_h, u_h), \xi_{\tilde{h}})\|_{\mathbf{H}\times Q} \\ &\quad \leqslant C h^r \{\|\boldsymbol{\sigma}\|_{[H^r(\Omega)]^2} + \|\operatorname{div} \boldsymbol{\sigma}\|_{H^r(\Omega)} + \|u\|_{H^{r+1}(\Omega)}\} + C \tilde{h}^r \|\xi\|_{H^{r+1/2}(\Gamma_{\mathrm{N}})}. \end{aligned}$$

Proof. It follows from the Cea estimate in Theorem 3.1 and the approximation properties of the subspaces M_h, X_h, and $Q_{\tilde{h}}$, respectively (see, e.g. [1,5,22]). □

4. A residual-based a posteriori error analysis

In this section, we proceed as in [19] and derive a reliable and efficient residual-based a posteriori error estimate for our augmented mixed finite element method. Let us first introduce some notations. Given $T \in \mathscr{T}_h$, we denote by $E(T)$ the set of its edges, and by E_h the set of all edges of the triangulation $\mathscr{T}_h$. Then we can write $E_h = E_h(\Omega) \cup E_h(\Gamma_{\mathrm{D}}) \cup E_h(\Gamma_{\mathrm{N}})$, where $E_h(\Omega) := \{e \in E_h : e \subseteq \Omega\}$, $E_h(\Gamma_{\mathrm{D}}) := \{e \in E_h : e \subseteq \Gamma_{\mathrm{D}}\}$, and similarly for $E_h(\Gamma_{\mathrm{N}})$. In what follows, h_T and h_e stand for the diameter of triangle $T \in \mathscr{T}_h$ and the length of edge $e \in E_h$, respectively. Further, for each $e \subseteq E_h(\Gamma_{\mathrm{N}})$ we set $\tilde{h}_e := |\tilde{\Gamma}_j|$, where $\tilde{\Gamma}_j$ is the segment containing edge e. Also, given a vector valued function $\boldsymbol{\tau} := (\tau_1, \tau_2)^{\mathrm{t}}$ defined in Ω, an edge $e \in E(T) \cap E_h(\Omega)$, and the unit tangential vector $\mathbf{t}_T$ along e, we let $J[\boldsymbol{\tau} \cdot \mathbf{t}_T]$ be the corresponding jump across e, that is $J[\boldsymbol{\tau} \cdot \mathbf{t}_T] := (\boldsymbol{\tau}_T - \boldsymbol{\tau}_{T'})|_e \cdot \mathbf{t}_T$, where T' is the other triangle of $\mathscr{T}_h$ having e as edge. Here, the tangential vector $\mathbf{t}_T$ is given by $(-v_2, v_1)^{\mathrm{t}}$ where $\boldsymbol{v}_T := (v_1, v_2)^t$ is the unit outward normal to ∂T. Finally, we let $\operatorname{curl}(\boldsymbol{\tau})$ be the scalar $\partial \tau_2 / \partial x_1 - \partial \tau_1 / \partial x_2$.

Now, let $I_h : H^1(\Omega) \to X_h$ be the usual Clément interpolation operator (see [12]). The following lemma states the local approximation properties of I_h.

Lemma 4.1. *There exist positive constants C_1 and C_2, independent of h, such that for all $\varphi \in H^1(\Omega)$ there holds*

$$\|\varphi - I_h(\varphi)\|_{0,T} \leqslant C_1 h_T \|\varphi\|_{1,\Delta(T)} \quad \forall T \in \mathcal{T}_h,$$

and

$$\|\varphi - I_h(\varphi)\|_{0,e} \leqslant C_2 h_e^{1/2} \|\varphi\|_{1,\Delta(e)} \quad \forall e \in E_h,$$

where $\Delta(T) := \cup\{T' \in \mathcal{T}_h : T' \cap T \neq \emptyset\}$ and $\Delta(e) := \cup\{T' \in \mathcal{T}_h : T' \cap e \neq \emptyset\}$.

Throughout the rest of the paper we assume that the Neumann datum $g \in L^2(\Gamma_{\mathrm{N}})$. The main result of the present section is summarized in the following theorem.

Theorem 4.1. *Let $((\boldsymbol{\sigma}, u), \xi) \in \mathbf{H} \times Q$ and $((\boldsymbol{\sigma}_h, u_h), \xi_{\tilde{h}}) \in \mathbf{H}_h \times Q_{\tilde{h}}$ be the unique solutions of the continuous and discrete formulations* (2.5) *and* (3.5), *respectively. Then there exist positive constants C_{eff}, C_{rel}, independent of h and $\tilde{h}$, such that*

$$C_{\mathrm{eff}}\, \boldsymbol{\eta}^2 \leqslant \|((\boldsymbol{\sigma} - \boldsymbol{\sigma}_h, u - u_h), \xi - \xi_{\tilde{h}})\|^2_{\mathbf{H}\times Q} \leqslant C_{\mathrm{rel}} \boldsymbol{\eta}^2, \tag{4.1}$$

where $\boldsymbol{\eta}^2 := \sum_{T\in\mathcal{T}_h} \eta_T^2$, and for each $T \in \mathcal{T}_h$ we define

$$\begin{aligned}\eta_T^2 := {} & \|f + \operatorname{div} \boldsymbol{\sigma}_h\|^2_{L^2(T)} + h_T^2 \|\nabla u_h - \boldsymbol{\sigma}_h\|^2_{[L^2(T)]^2} + \sum_{e\in E(T)\cap E_h(\Gamma_{\mathrm{N}})} h_e \left\| \frac{\mathrm{d}u_h}{\mathrm{d}\mathbf{t}_T} + \frac{\mathrm{d}\xi_{\tilde{h}}}{\mathrm{d}\mathbf{t}_T} \right\|^2_{L^2(e)} \\ & + \sum_{e\in E(T)\cap E_h(\Omega)} h_e \|J[(\boldsymbol{\sigma}_h - \nabla u_h)\cdot \mathbf{t}_T]\|^2_{L^2(e)} + \sum_{e\in E(T)\cap E_h(\Gamma)} h_e \|(\boldsymbol{\sigma}_h - \nabla u_h)\cdot \mathbf{t}_T\|^2_{L^2(e)} \\ & + \log[1 + C_{\tilde{h}}(\Gamma_{\mathrm{N}})] \sum_{e\in E(T)\cap E_h(\Gamma_{\mathrm{N}})} \tilde{h}_e \|g - \boldsymbol{\sigma}_h \cdot \boldsymbol{\nu}\|^2_{L^2(e)},\end{aligned} \tag{4.2}$$

with $C_{\tilde{h}}(\Gamma_{\mathrm{N}}) := \max\{|\tilde{\Gamma}_i|/|\tilde{\Gamma}_j| : \ |i-j| = 1, i, j \in \{1, \ldots, m\}\}$.

The proof of Theorem 4.1 is separated into the three parts given by the next subsections.

4.1. *Estimate for* $\|(\boldsymbol{\sigma} - \boldsymbol{\sigma}_h, u - u_h)\|_{\mathbf{H}}$

We first define the spaces $H_0 := \{\boldsymbol{\tau} \in H(\operatorname{div}; \Omega) : \operatorname{div} \boldsymbol{\tau} = 0 \text{ in } \Omega,\ \boldsymbol{\tau}\cdot\boldsymbol{\nu} = 0 \text{ on } \Gamma_{\mathrm{N}}\}$ and $\mathbf{H}_0 := H_0 \times H^1_{\Gamma_{\mathrm{D}}}(\Omega)$. Then, we have the following preliminary result.

Lemma 4.2. *There exists $C > 0$, independent of h, such that*

$$\begin{aligned}& C\|(\boldsymbol{\sigma} - \boldsymbol{\sigma}_h, u - u_h)\|_{\mathbf{H}} \\ & \quad \leqslant \sup_{\substack{(\boldsymbol{\tau},v)\in\mathbf{H}_0 \\ (\boldsymbol{\tau},v)\neq 0}} \frac{A((\boldsymbol{\sigma} - \boldsymbol{\sigma}_h, u - u_h), (\boldsymbol{\tau}, v))}{\|(\boldsymbol{\tau}, v)\|_{\mathbf{H}}} + \|f + \operatorname{div} \boldsymbol{\sigma}_h\|_{L^2(\Omega)} + \|g - \boldsymbol{\sigma}_h\cdot\boldsymbol{\nu}\|_{H^{-1/2}(\Gamma_{\mathrm{N}})}.\end{aligned}$$

Proof. Let $\boldsymbol{\sigma}^* := \nabla z \in H(\operatorname{div}; \Omega)$, where $z \in H^1(\Omega)$ is the weak solution of the boundary value problem:

$$-\Delta z = f + \operatorname{div} \boldsymbol{\sigma}_h \quad \text{in } \Omega, \qquad z = 0 \quad \text{on } \Gamma_{\mathrm{D}}, \qquad \frac{\partial z}{\partial \boldsymbol{\nu}} = g - \boldsymbol{\sigma}_h\cdot\boldsymbol{\nu} \quad \text{on } \Gamma_{\mathrm{N}}.$$

It follows that $\operatorname{div} \boldsymbol{\sigma}^* = -(f + \operatorname{div} \boldsymbol{\sigma}_h)$ in Ω and $\boldsymbol{\sigma}^*\cdot\boldsymbol{\nu} = g - \boldsymbol{\sigma}_h\cdot\boldsymbol{\nu}$ on Γ_{N}, whence $(\boldsymbol{\sigma} - \boldsymbol{\sigma}_h - \boldsymbol{\sigma}^*)$ belongs to H_0. In addition, the corresponding continuous dependence result yields the existence of a constant $C > 0$ such that

$$\|\boldsymbol{\sigma}^*\|_{H(\operatorname{div};\Omega)} \leqslant C\{\|f + \operatorname{div} \boldsymbol{\sigma}_h\|_{L^2(\Omega)} + \|g - \boldsymbol{\sigma}_h\cdot\boldsymbol{\nu}\|_{H^{-1/2}(\Gamma_{\mathrm{N}})}\}. \tag{4.3}$$

Now, using the strong coerciveness (cf. (2.12)) and boundedness of A, we find that

$$\begin{aligned}\tfrac{1}{2}\|(\boldsymbol{\sigma}-\boldsymbol{\sigma}_h-\boldsymbol{\sigma}^*,u-u_h)\|_{\mathbf{H}}^2 &\leqslant A((\boldsymbol{\sigma}-\boldsymbol{\sigma}-\boldsymbol{\sigma}^*,u-u_h),(\boldsymbol{\sigma}-\boldsymbol{\sigma}_h-\boldsymbol{\sigma}^*,u-u_h))\\ &= A((\boldsymbol{\sigma}-\boldsymbol{\sigma}_h,u-u_h),(\boldsymbol{\sigma}-\boldsymbol{\sigma}_h-\boldsymbol{\sigma}^*,u-u_h)) - A((\boldsymbol{\sigma}^*,0),(\boldsymbol{\sigma}-\boldsymbol{\sigma}_h-\boldsymbol{\sigma}^*,u-u_h))\\ &\leqslant A((\boldsymbol{\sigma}-\boldsymbol{\sigma}_h,u-u_h),(\boldsymbol{\sigma}-\boldsymbol{\sigma}_h-\boldsymbol{\sigma}^*,u-u_h)) + \|A\|\|\boldsymbol{\sigma}^*\|_{H(\mathrm{div};\Omega)}\|(\boldsymbol{\sigma}-\boldsymbol{\sigma}_h-\boldsymbol{\sigma}^*,u-u_h)\|_{\mathbf{H}}\end{aligned}$$

which, dividing by $\|(\boldsymbol{\sigma}-\boldsymbol{\sigma}_h-\boldsymbol{\sigma}^*,u-u_h)\|_{\mathbf{H}}$, and then taking supremum on $\mathbf{H}_0$, implies

$$C\|(\boldsymbol{\sigma}-\boldsymbol{\sigma}_h-\boldsymbol{\sigma}^*,u-u_h)\|_{\mathbf{H}} \leqslant \sup_{\substack{(\boldsymbol{\tau},v)\in\mathbf{H}_0\\(\boldsymbol{\tau},v)\neq 0}} \frac{A((\boldsymbol{\sigma}-\boldsymbol{\sigma}_h,u-u_h),(\boldsymbol{\tau},v))}{\|(\boldsymbol{\tau},v)\|_{\mathbf{H}}} + \|\boldsymbol{\sigma}^*\|_{H(\mathrm{div};\Omega)}. \tag{4.4}$$

Finally, triangle inequality gives $\|(\boldsymbol{\sigma}-\boldsymbol{\sigma}_h,u-u_h)\|_{\mathbf{H}}\leqslant\|(\boldsymbol{\sigma}-\boldsymbol{\sigma}_h-\boldsymbol{\sigma}^*,u-u_h)\|_{\mathbf{H}}+\|\boldsymbol{\sigma}^*\|_{H(\mathrm{div};\Omega)}$, which, together with the estimates (4.4) and (4.3), completes the proof. □

The corresponding upper bound for the supremum appearing in Lemma 4.2 is provided next.

Lemma 4.3. *There exists $C>0$, independent of h and $\tilde{h}$, such that*

$$\sup_{\substack{(\boldsymbol{\tau},v)\in\mathbf{H}_0\\(\boldsymbol{\tau},v)\neq 0}} \frac{A((\boldsymbol{\sigma}-\boldsymbol{\sigma}_h,u-u_h),(\boldsymbol{\tau},v))}{\|(\boldsymbol{\tau},v)\|_{\mathbf{H}}} \leqslant C\left\{\sum_{T\in\mathscr{T}_h}\tilde{\eta}_T^2\right\}^{1/2},$$

where for any triangle $T\in\mathscr{T}_h$ we define

$$\begin{aligned}\tilde{\eta}_T^2 := {}& h_T^2\|f+\mathrm{div}\,\boldsymbol{\sigma}_h\|_{L^2(T)}^2 + h_T^2\|\nabla u_h-\boldsymbol{\sigma}_h\|_{[L^2(T)]^2}^2 + \sum_{e\in E(T)\cap E_h(\Omega)} h_e\|J[(\boldsymbol{\sigma}_h-\nabla u_h)\cdot\mathbf{t}_T]\|_{L^2(e)}^2\\ &+ \sum_{e\in E(T)\cap E_h(\Gamma)} h_e\|(\boldsymbol{\sigma}_h-\nabla u_h)\cdot\mathbf{t}_T\|_{L^2(e)}^2 + \sum_{e\in E(T)\cap E_h(\Gamma_{\mathrm{N}})} h_e\left\|\frac{\mathrm{d}u_h}{\mathrm{d}\mathbf{t}_T}+\frac{\mathrm{d}\xi_{\tilde{h}}}{\mathrm{d}\mathbf{t}_T}\right\|_{L^2(e)}^2.\end{aligned} \tag{4.5}$$

Proof. Let $(\boldsymbol{\tau},v)\in\mathbf{H}_0$ such that $(\boldsymbol{\tau},v)\neq 0$. Since $\mathrm{div}(\boldsymbol{\tau})=0$ in Ω and Ω is connected, there exists a stream function $\varphi\in H^1(\Omega)$ such that $\int_\Omega\varphi=0$ and

$$\boldsymbol{\tau}=\mathbf{curl}(\varphi):=\begin{pmatrix}-\dfrac{\partial\varphi}{\partial x_2}\\[2mm]\dfrac{\partial\varphi}{\partial x_1}\end{pmatrix}.$$

Then, denoting by v_h and φ_h the Clément interpolants of v and φ, respectively, and defining $\boldsymbol{\tau}_h:=\mathbf{curl}\,\varphi_h$, we obtain $\boldsymbol{\tau}_h\in M_h$, $\mathrm{div}\,\boldsymbol{\tau}_h=0$ in Ω, and $\boldsymbol{\tau}-\boldsymbol{\tau}_h=\mathbf{curl}(\varphi-\varphi_h)$.

Next, from the first equations of (2.5) and (3.5) we find that

$$A((\boldsymbol{\sigma},u),(\boldsymbol{\tau}-\boldsymbol{\tau}_h,v-v_h)) = F(\boldsymbol{\tau}-\boldsymbol{\tau}_h,v-v_h) - B((\boldsymbol{\tau}-\boldsymbol{\tau}_h,v-v_h),\xi)$$

and

$$A((\boldsymbol{\sigma}-\boldsymbol{\sigma}_h,u-u_h),(\boldsymbol{\tau}_h,v_h)) = -B((\boldsymbol{\tau}_h,v_h),\xi-\xi_{\tilde{h}}),$$

which gives

$$\begin{aligned}&A((\boldsymbol{\sigma}-\boldsymbol{\sigma}_h,u-u_h),(\boldsymbol{\tau},v))\\ &\quad= A((\boldsymbol{\sigma}-\boldsymbol{\sigma}_h,u-u_h),(\boldsymbol{\tau}-\boldsymbol{\tau}_h,v-v_h)) + A((\boldsymbol{\sigma}-\boldsymbol{\sigma}_h,u-u_h),(\boldsymbol{\tau}_h,v_h))\\ &\quad= F(\boldsymbol{\tau}-\boldsymbol{\tau}_h,v-v_h) - B((\boldsymbol{\tau}-\boldsymbol{\tau}_h,v-v_h),\xi) - A((\boldsymbol{\sigma}_h,u_h),(\boldsymbol{\tau}-\boldsymbol{\tau}_h,v-v_h)) - B((\boldsymbol{\tau}_h,v_h),\xi-\xi_{\tilde{h}}).\end{aligned}$$

It follows, employing the definitions of F and B (cf. (2.7), (2.8)), and using that $\boldsymbol{\tau}\cdot\boldsymbol{v}=0$ on Γ_{N}, that

$$A((\boldsymbol{\sigma}-\boldsymbol{\sigma}_h, u-u_h),(\boldsymbol{\tau}, v)) = \int_\Omega f(v-v_h) - \langle(\boldsymbol{\tau}-\boldsymbol{\tau}_h)\cdot\boldsymbol{v}, \xi_{\tilde h}\rangle_{\Gamma_{\mathrm{N}}} - A((\boldsymbol{\sigma}_h, u_h),(\boldsymbol{\tau}-\boldsymbol{\tau}_h, v-v_h)).$$

Next, developing $A((\boldsymbol{\sigma}_h, u_h),(\boldsymbol{\tau}-\boldsymbol{\tau}_h, v-v_h))$ (see (2.6)), integrating by parts in Ω, using that $u_h=0$ on Γ_{D} and that $\operatorname{div}(\boldsymbol{\tau}-\boldsymbol{\tau}_h)=0$ in Ω, and reordering the resulting terms, we arrive to

$$\begin{aligned} A((\boldsymbol{\sigma}-\boldsymbol{\sigma}_h, u-u_h),(\boldsymbol{\tau}, v)) &= \int_\Omega (f+\operatorname{div}\boldsymbol{\sigma}_h)(v-v_h) - \langle \mathbf{curl}(\varphi-\varphi_h)\cdot\boldsymbol{v}, u_h+\xi_{\tilde h}\rangle_{\Gamma_{\mathrm{N}}} \\ &\quad - \frac{1}{2}\int_\Omega (\boldsymbol{\sigma}_h-\nabla u_h)\cdot\mathbf{curl}(\varphi-\varphi_h) - \frac{1}{2}\int_\Omega (\nabla u_h-\boldsymbol{\sigma}_h)\cdot\nabla(v-v_h). \end{aligned} \tag{4.6}$$

We now proceed to derive suitable bounds for each one of the terms on the right-hand side of (4.6). We first observe that $\mathbf{curl}(\varphi-\varphi_h)\cdot\boldsymbol{v} = -\mathrm{d}(\varphi-\varphi_h)/\mathrm{d}\mathbf{t}_T$, and hence

$$\begin{aligned} \langle \mathbf{curl}(\varphi-\varphi_h)\cdot\boldsymbol{v}, u_h+\xi_{\tilde h}\rangle_{\Gamma_{\mathrm{N}}} &= \left\langle \varphi-\varphi_h, \frac{\mathrm{d}u_h}{\mathrm{d}\mathbf{t}_T} + \frac{\mathrm{d}\xi_{\tilde h}}{\mathrm{d}\mathbf{t}_T}\right\rangle_{\Gamma_{\mathrm{N}}} \\ &= \sum_{T\in\mathscr{T}_h}\sum_{e\in E(T)\cap E_h(\Gamma_{\mathrm{N}})} \left\langle \varphi-\varphi_h, \frac{\mathrm{d}u_h}{d\mathbf{t}_T} + \frac{\mathrm{d}\xi_{\tilde h}}{\mathrm{d}\mathbf{t}_T}\right\rangle_{L^2(e)}. \end{aligned} \tag{4.7}$$

Also, using that

$$\int_\Omega = \sum_{T\in\mathscr{T}_h}\int_T,$$

integrating by parts, and noting that $\operatorname{curl}(\boldsymbol{\sigma}_h-\nabla u_h)=0$ in each $T\in\mathscr{T}_h$, we deduce that

$$\begin{aligned} \int_\Omega (\boldsymbol{\sigma}_h-\nabla u_h)\cdot\mathbf{curl}(\varphi-\varphi_h) &= \frac{1}{2}\sum_{T\in\mathscr{T}_h}\sum_{e\in E(T)\cap E_h(\Omega)} \langle J[\boldsymbol{\sigma}_h-\nabla u_h]\cdot\mathbf{t}_T, \varphi-\varphi_h\rangle_{L^2(e)} \\ &\quad + \sum_{T\in\mathscr{T}_h}\sum_{e\in E(T)\cap E_h(\Gamma)} \langle(\boldsymbol{\sigma}_h-\nabla u_h)\cdot\mathbf{t}_T, \varphi-\varphi_h\rangle_{L^2(e)}. \end{aligned} \tag{4.8}$$

Then, applying Cauchy–Schwarz inequality, the estimates from Lemma 4.1, and the fact that the number of triangles in $\Delta(T)$ and $\Delta(e)$ are bounded, we obtain that the terms in (4.6)–(4.8), respectively, are bounded as follows:

$$\left|\int_\Omega (f+\operatorname{div}\boldsymbol{\sigma}_h)(v-v_h)\right| \leqslant C\left\{\sum_{T\in\mathscr{T}_h} h_T^2\|f+\operatorname{div}\boldsymbol{\sigma}_h\|_{L^2(T)}^2\right\}^{1/2}\|v\|_{H^1(\Omega)}, \tag{4.9}$$

$$\left|\int_\Omega (\nabla u_h-\boldsymbol{\sigma}_h)\cdot\nabla(v-v_h)\right| \leqslant C\left\{\sum_{T\in\mathscr{T}_h} h_T^2\|\nabla u_h-\boldsymbol{\sigma}_h\|_{[L^2(T)]^2}^2\right\}^{1/2}\|v\|_{H^1(\Omega)}, \tag{4.10}$$

$$|\langle \mathbf{curl}(\varphi-\varphi_h)\cdot\boldsymbol{v}, u_h+\xi_{\tilde h}\rangle_{\Gamma_{\mathrm{N}}}| \leqslant C\left\{\sum_{T\in\mathscr{T}_h}\sum_{e\in E(T)\cap E_h(\Gamma_{\mathrm{N}})} h_e\left\|\frac{\mathrm{d}u_h}{\mathrm{d}\mathbf{t}_T}+\frac{\mathrm{d}\xi_{\tilde h}}{\mathrm{d}\mathbf{t}_T}\right\|_{L^2(e)}^2\right\}^{1/2}\|\varphi\|_{H^1(\Omega)}, \tag{4.11}$$

$$\begin{aligned} &\left|\sum_{T\in\mathscr{T}_h}\sum_{e\in E(T)\cap E_h(\Omega)} \langle J[\boldsymbol{\sigma}_h-\nabla u_h]\cdot\mathbf{t}_T, \varphi-\varphi_h\rangle_{L^2(e)}\right| \\ &\quad \leqslant C\left\{\sum_{T\in\mathscr{T}_h}\sum_{e\in E(T)\cap E_h(\Omega)} h_e\|J[\boldsymbol{\sigma}_h-\nabla u_h]\cdot\mathbf{t}_T\|_{L^2(e)}^2\right\}^{1/2}\|\varphi\|_{H^1(\Omega)}, \end{aligned} \tag{4.12}$$

and

$$\left|\sum_{T\in\mathcal{T}_h}\sum_{e\in E(T)\cap E_h(\Gamma)}\langle(\boldsymbol{\sigma}_h-\nabla u_h)\cdot\mathbf{t}_T,\varphi-\varphi_h\rangle_{L^2(e)}\right|$$
$$\leqslant C\left\{\sum_{T\in\mathcal{T}_h}\sum_{e\in E(T)\cap E_h(\Gamma)}h_e\|(\boldsymbol{\sigma}_h-\nabla u_h)\cdot\mathbf{t}_T\|_{L^2(e)}^2\right\}^{1/2}\|\varphi\|_{H^1(\Omega)}. \tag{4.13}$$

Since $\int_\Omega\varphi=0$ and $\mathbf{curl}(\varphi)=\boldsymbol{\tau}$, we clearly have $\|\varphi\|_{H^1(\Omega)}\leqslant C|\varphi|_{H^1(\Omega)}=C\|\boldsymbol{\tau}\|_{L^2(\Omega)}=C\|\boldsymbol{\tau}\|_{H(\mathrm{div};\Omega)}$. Therefore, using this norm estimate in (4.11)–(4.13), and replacing (4.9) up to (4.13) back into (4.6), we obtain the required inequality and conclude the proof. □

We can establish now our a posteriori error estimate for $\|(\boldsymbol{\sigma}-\boldsymbol{\sigma}_h,u-u_h)\|_{\mathbf{H}}$.

Theorem 4.2. *There exists $C>0$, independent of h and $\tilde{h}$, such that*

$$\|(\boldsymbol{\sigma}-\boldsymbol{\sigma}_h,u-u_h)\|_{\mathbf{H}}\leqslant C\left\{\sum_{T\in\mathcal{T}_h}\eta_T^2\right\}^{1/2},$$

where η_T^2 is given by (4.2) *for each $T\in\mathcal{T}_h$.*

Proof. We see from Lemma 4.2 that it just remains to estimate the residuals $\|f+\mathrm{div}\boldsymbol{\sigma}_h\|_{L^2(\Omega)}$ and $\|g-\boldsymbol{\sigma}_h\cdot\boldsymbol{v}\|^2_{H^{-1/2}(\Gamma_\mathrm{N})}$ in terms of local quantities. For the first expression we simply write

$$\|f+\mathrm{div}\,\boldsymbol{\sigma}_h\|^2_{L^2(\Omega)}=\sum_{T\in\mathcal{T}_h}\|f+\mathrm{div}\,\boldsymbol{\sigma}_h\|^2_{L^2(T)}, \tag{4.14}$$

and for the second one we apply Theorem 2 in [9] to yield

$$\|g-\boldsymbol{\sigma}_h\cdot\boldsymbol{v}\|^2_{H^{-1/2}(\Gamma_\mathrm{N})}\leqslant C\,\log[1+C_{\tilde{h}}(\Gamma_\mathrm{N})]\sum_{j=1}^m|\tilde{\Gamma}_j|\|g-\boldsymbol{\sigma}_h\cdot\boldsymbol{v}\|^2_{L^2(\tilde{\Gamma}_j)}, \tag{4.15}$$

where $C_{\tilde{h}}(\Gamma_\mathrm{N}):=\max\{|\tilde{\Gamma}_i|/|\tilde{\Gamma}_j|:\ |i-j|=1,i,j\in\{1,\ldots,m\}\}$. Then, since each edge of $E_h(\Gamma_\mathrm{N})$ is contained in a segment $\tilde{\Gamma}_j$ for some $j\in\{1,\ldots,m\}$, we deduce that

$$\sum_{j=1}^m|\tilde{\Gamma}_j|\|g-\boldsymbol{\sigma}_h\cdot\boldsymbol{v}\|^2_{L^2(\tilde{\Gamma}_j)}=\sum_{e\in E_h(\Gamma_\mathrm{N})}\tilde{h}_e\|g-\boldsymbol{\sigma}_h\cdot\boldsymbol{v}\|^2_{L^2(e)}, \tag{4.16}$$

which is replaced back into (4.15). The rest of the proof follows from Lemmata 4.2 and 4.3, and the estimates (4.14) and (4.15). We omit further details. □

4.2. Estimate for $\|\xi-\xi_{\tilde{h}}\|_Q$

The a posteriori error estimate for the Lagrange multiplier ξ is provided next.

Theorem 4.3. *There exists $C>0$, independent of h and $\tilde{h}$, such that*

$$\|\xi-\xi_{\tilde{h}}\|_{H^{1/2}_{00}(\Gamma_\mathrm{N})}\leqslant C\left\{\sum_{T\in\mathcal{T}_h}\eta_T^2\right\}^{1/2},$$

where η_T is given by (4.2).

Proof. According to the inf–sup condition (2.11), we can write

$$\|\xi-\xi_{\tilde{h}}\|_{H_{00}^{1/2}(\Gamma_{\mathrm{N}})} \leqslant C \sup_{\substack{\tau\in H(\mathrm{div};\Omega)\\ \mathrm{div}\,\tau=0,\tau\neq 0}} \frac{\langle \tau\cdot\nu,\xi\rangle_{\Gamma_{\mathrm{N}}}-\langle \tau\cdot\nu,\xi_{\tilde{h}}\rangle_{\Gamma_{\mathrm{N}}}}{\|\tau\|_{H(\mathrm{div};\Omega)}}. \tag{4.17}$$

Now, given $\tau\in H(\mathrm{div};\Omega)$ with $\mathrm{div}\,\tau=0$ in Ω, we observe from the first equation of (2.5) that $\langle \tau\cdot\nu,\xi\rangle_{\Gamma_{\mathrm{N}}} = -A((\sigma,u),(\tau,0))$. Also, since Ω is connected, there exists $\varphi\in H^1(\Omega)$ such that $\int_\Omega \varphi=0$ and $\tau=\mathbf{curl}\,\varphi$. Next, as in the proof of Lemma 4.3, we let φ_h be the Clément interpolant of φ and define $\tau_h:=\mathbf{curl}\,\varphi_h$. It is clear that $\tau_h\in M_h$ and $\mathrm{div}\,\tau_h=0$ in Ω, and hence, the first equation of (3.5) gives $\langle \tau_h\cdot\nu,\xi_{\tilde{h}}\rangle_{\Gamma_{\mathrm{N}}}=-A((\sigma_h,u_h),(\tau_h,0))$.

It follows that

$$\begin{aligned}\langle \tau\cdot\nu,\xi\rangle_{\Gamma_{\mathrm{N}}}-\langle \tau\cdot\nu,\xi_{\tilde{h}}\rangle_{\Gamma_{\mathrm{N}}} &= -A((\sigma,u),(\tau,0))-\langle(\tau-\tau_h)\cdot\nu,\xi_{\tilde{h}}\rangle_{\Gamma_{\mathrm{N}}}+A((\sigma_h,u_h),(\tau_h,0))\\ &= -A((\sigma,u)-(\sigma_h,u_h),(\tau,0))-A((\sigma_h,u_h),((\tau-\tau_h),0))-\langle(\tau-\tau_h)\cdot\nu,\xi_{\tilde{h}}\rangle_{\Gamma_{\mathrm{N}}},\end{aligned}$$

which, developing $A((\sigma_h,u_h),((\tau-\tau_h),0))$ (see (2.6)), integrating by parts in Ω, using that $u_h=0$ on Γ_{D} and that $\mathrm{div}(\tau-\tau_h)=0$ in Ω, and finally replacing $(\tau-\tau_h)$ by $\mathbf{curl}(\varphi-\varphi_h)$, leads to

$$\begin{aligned}\langle \tau\cdot\nu,\xi\rangle_{\Gamma_{\mathrm{N}}}-\langle \tau\cdot\nu,\xi_{\tilde{h}}\rangle_{\Gamma_{\mathrm{N}}} &= -A((\sigma,u)-(\sigma_h,u_h),(\tau,0))\\ &\quad -\langle \mathbf{curl}(\varphi-\varphi_h)\cdot\nu,u_h+\xi_{\tilde{h}}\rangle_{\Gamma_{\mathrm{N}}}-\frac{1}{2}\int_\Omega(\sigma_h-\nabla u_h)\cdot\mathbf{curl}(\varphi-\varphi_h).\end{aligned} \tag{4.18}$$

Therefore, using the boundedness of A for the first term on the right-hand side of (4.18), proceeding as in (4.8) for the third one, and then applying the upper bounds provided by (4.11)–(4.13), we conclude that

$$\frac{|\langle \tau\cdot\nu,\xi\rangle_{\Gamma_{\mathrm{N}}}-\langle \tau\cdot\nu,\xi_{\tilde{h}}\rangle_{\Gamma_{\mathrm{N}}}|}{\|\tau\|_{H(\mathrm{div};\Omega)}} \leqslant C\left\{\|(\sigma-\sigma_h,u-u_h)\|_{\mathbf{H}}^2+\sum_{T\in\mathscr{T}_h}\bar{\eta}_T^2\right\}^{1/2}, \tag{4.19}$$

where

$$\bar{\eta}_T^2=\tilde{\eta}_T^2-h_T^2\|f+\mathrm{div}\,\sigma_h\|_{L^2(T)}^2-h_T^2\|\nabla u_h-\sigma_h\|_{L^2(T)}^2,$$

with $\tilde{\eta}_T^2$ given by (4.5). In this way, (4.17), (4.19), and the a posteriori error estimate for $\|(\sigma-\sigma_h,u-u_h)\|_{\mathbf{H}}$ (cf. Theorem 4.2) complete the proof. □

Consequently, the reliability of the a posteriori error estimate, which is given by the upper bound in (4.1), follows directly from Theorems 4.2 and 4.3.

4.3. *Efficiency of the a posteriori error estimate*

In this subsection we follow the approach from [17] (see also [19]) to derive the lower bound in (4.1), which shows the efficiency of the a posteriori error estimate. We first recall from [24] that given $k\in\mathbb{N}$, $T\in\mathscr{T}_h$, and $e\in E(T)$, there exists an extension operator $L: C(e)\to C(T)$ that satisfies $L(p)\in\mathbf{P}_k(T)$ and $L(p)|_e=p\ \forall p\in\mathbf{P}_k(e)$. In addition, we define $w_e:=\bigcup\{T'\in\mathscr{T}_h: e\in E(T')\}$ and let ψ_T and ψ_e be the usual triangle-bubble and edge-bubble functions, respectively (see (1.5) and (1.6) in [25]), which satisfy $\mathrm{supp}(\psi_T)\subseteq T$, $\psi_T\in\mathbf{P}_3(T)$, $\psi_T=0$ on ∂T, $0\leqslant\psi_T\leqslant 1$ in T, $\mathrm{supp}(\psi_e)\subseteq w_e$, $\psi_e|_T\in\mathbf{P}_2(T)\ \forall T\subseteq w_e$, $\psi_e=0$ on $\partial T\backslash e$, and $0\leqslant\psi_e\leqslant 1$ in w_e. Additional properties of ψ_T, ψ_e, and L are collected in the following lemma.

Lemma 4.4. *There exist positive constants* c_1, c_2, *and* c_3, *depending only on k and the shape of the triangles, such that for all* $q \in \mathbf{P}_k(T)$ *and* $p \in \mathbf{P}_k(e)$, *there hold*

$$\|\psi_e L(p)\|^2_{L^2(e)} \leqslant \|p\|^2_{L^2(e)} \leqslant c_1 \|\psi_e^{1/2} p\|^2_{L^2(e)}, \tag{4.20}$$

$$c_2 h_e \|p\|^2_{L^2(e)} \leqslant \|\psi_e^{1/2} L(p)\|^2_{L^2(T)} \leqslant c_3 h_e \|p\|^2_{L^2(e)}. \tag{4.21}$$

Proof. See Lemma 4.1 in [24]. □

For the first term in (4.2) we use that $\operatorname{div} \boldsymbol{\sigma} = -f$ in Ω and write

$$\sum_{T \in \mathscr{T}_h} \|f + \operatorname{div} \boldsymbol{\sigma}_h\|^2_{L^2(T)} = \|\operatorname{div}(\boldsymbol{\sigma} - \boldsymbol{\sigma}_h)\|^2_{L^2(\Omega)}. \tag{4.22}$$

The corresponding estimate for the second term is also easily obtained. In fact, adding and subtracting $\boldsymbol{\sigma} = \nabla u$, we get

$$h_T^2 \|\nabla u_h - \boldsymbol{\sigma}_h\|^2_{[L^2(T)]^2} \leqslant C \|\nabla u_h - \boldsymbol{\sigma}_h\|^2_{[L^2(T)]^2} \leqslant C \left\{ |u - u_h|^2_{H^1(T)} + \|\boldsymbol{\sigma} - \boldsymbol{\sigma}_h\|^2_{[L^2(T)]^2} \right\},$$

whence

$$\sum_{T \in \mathscr{T}_h} h_T^2 \|\nabla u_h - \boldsymbol{\sigma}_h\|^2_{[L^2(T)]^2} \leqslant C \left\{ |u - u_h|^2_{H^1(\Omega)} + \|\boldsymbol{\sigma} - \boldsymbol{\sigma}_h\|^2_{[L^2(\Omega)]^2} \right\}. \tag{4.23}$$

The third term in (4.2) is bounded next.

Lemma 4.5. *There exists* $C > 0$, *independent of h and* $\tilde{h}$, *such that*

$$\sum_{e \in E_h(\Gamma_{\mathrm{N}})} h_e \left\| \frac{\mathrm{d}u_h}{\mathrm{d}\mathbf{t}_T} + \frac{\mathrm{d}\xi_{\tilde{h}}}{\mathrm{d}\mathbf{t}_T} \right\|^2_{L^2(e)} \leqslant C \left\{ \|\xi - \xi_{\tilde{h}}\|^2_{H^{1/2}_{00}(\Gamma_{\mathrm{N}})} + \|u - u_h\|^2_{H^1(\Omega)} \right\}. \tag{4.24}$$

Proof. Let us define $v_e := \mathrm{d}u_h/\mathrm{d}\mathbf{t}_T + \mathrm{d}\xi_{\tilde{h}}/\mathrm{d}\mathbf{t}_T$ on $e \in E_h(\Gamma_{\mathrm{N}})$. Then, using that $u = -\xi$ on Γ_{N}, we can write $v_e = (\mathrm{d}/\mathrm{d}\mathbf{t}_T)(u_h - u) + (\mathrm{d}/\mathrm{d}\mathbf{t}_T)(\xi_{\tilde{h}} - \xi)$ on e. Hence, applying (4.20), we obtain that

$$h_e \|v_e\|^2_{L^2(e)} \leqslant c_1 \left\{ h_e \int_e \psi_e v_e \frac{\mathrm{d}}{\mathrm{d}\mathbf{t}_T}(u_h - u) + h_e \int_e \psi_e v_e \frac{\mathrm{d}}{\mathrm{d}\mathbf{t}_T}(\xi_{\tilde{h}} - \xi) \right\}. \tag{4.25}$$

We now define the function $\psi := h_e \psi_e v_e$ on each $e \in E_h(\Gamma_{\mathrm{N}})$, and introduce the trivial extensions

$$\hat{\psi} := \begin{cases} \psi & \text{on } \Gamma_{\mathrm{N}} \\ 0 & \text{on } \Gamma_{\mathrm{D}} \end{cases}$$

and

$$\hat{\xi} := \begin{cases} \xi_{\tilde{h}} - \xi & \text{on } \Gamma_{\mathrm{N}} \\ 0 & \text{on } \Gamma_{\mathrm{D}}. \end{cases}$$

Since ψ and $(\xi_{\tilde{h}} - \xi)$ belong to $H^{1/2}_{00}(\Gamma_{\mathrm{N}})$, it follows that $\hat{\psi}$ and $\hat{\xi}$ lie in $H^{1/2}(\Gamma)$ and that $\|\hat{\psi}\|_{H^{1/2}(\Gamma)}$ and $\|\hat{\xi}\|_{H^{1/2}(\Gamma)}$ are equivalent to $\|\psi\|_{H^{1/2}_{00}(\Gamma_{\mathrm{N}})}$ and $\|\xi_{\tilde{h}} - \xi\|_{H^{1/2}_{00}(\Gamma_{\mathrm{N}})}$, respectively.

Thus, applying the inverse inequality to the piecewise polynomial $\hat{\psi}$, using the boundedness of the tangential derivative, noting that $0 \leqslant \psi_e \leqslant 1$, $h_e \leqslant h$, and that $u_h = u = 0$ on Γ_{D}, and employing the usual trace Theorem, we deduce that

$$\sum_{e\in E_h(\Gamma_{\mathrm N})} h_e \int_e \psi_e v_e \frac{\mathrm d}{\mathrm d\mathbf t_T}(u_h-u) = \int_\Gamma \hat\psi \frac{\mathrm d}{\mathrm d\mathbf t_T}(u_h-u) \leqslant \|\hat\psi\|_{H^{1/2}(\Gamma)} \left\| \frac{\mathrm d}{\mathrm d\mathbf t_T}(u_h-u)\right\|_{H^{-1/2}(\Gamma)}$$
$$\leqslant C h^{-1/2}\|\hat\psi\|_{L^2(\Gamma)}\|u-u_h\|_{H^{1/2}(\Gamma)}$$
$$\leqslant C\left\{\sum_{e\in E_h(\Gamma_{\mathrm N})} h_e\|v_e\|^2_{L^2(e)}\right\}^{1/2} \|u-u_h\|_{H^1(\Omega)}. \tag{4.26}$$

Proceeding similarly as for the above estimate (see also [17, proof of Lemma 5.7]), using now the extension $\hat\xi$, we find that there exists $C>0$, independent of h and $\tilde h$, such that

$$\sum_{e\in E_h(\Gamma_{\mathrm N})} h_e \int_e \psi_e v_e \frac{\mathrm d}{\mathrm d\mathbf t_T}(\xi_{\tilde h}-\xi) \leqslant C\left\{\sum_{e\in E_h(\Gamma_{\mathrm N})} h_e\|v_e\|^2_{L^2(e)}\right\}^{1/2} \|\xi_{\tilde h}-\xi\|_{H^{1/2}_{00}(\Gamma_{\mathrm N})}. \tag{4.27}$$

Therefore, (4.24) is a consequence of (4.25)–(4.27). □

The following technical lemma is needed to bound the fourth and fifth terms in (4.2).

Lemma 4.6. *There exists $c>0$, independent of h and $\tilde h$, such that for each $e\in E_h$ there holds*

$$h_e\|\hat J_e[(\boldsymbol\sigma_h-\nabla u_h)\cdot\mathbf t_T]\|^2_{L^2(e)} \leqslant c\|\boldsymbol\sigma_h-\nabla u_h\|^2_{[L^2(w_e)]^2}, \tag{4.28}$$

where

$$\hat J_e[(\boldsymbol\sigma_h-\nabla u_h)\cdot\mathbf t_T] := \begin{cases} J[(\boldsymbol\sigma_h-\nabla u_h)\cdot\mathbf t_T] & \text{if } e\in E_h(\Omega),\\ (\boldsymbol\sigma_h-\nabla u_h)\cdot\mathbf t_T & \text{if } e\in E_h(\Gamma).\end{cases}$$

Proof. We adapt the proof of Lemma 6.2 in [10]. To this end, we first define the function $v_e := \hat J_e[(\boldsymbol\sigma_h-\nabla u_h)\cdot\mathbf t_T]$ on each $e\in E_h$. Then, (4.20) and the fact that $L(v_e)=v_e$ on e, yield

$$c_1^{-1}\|v_e\|^2_{L^2(e)} \leqslant \|\psi_e^{1/2}v_e\|^2_{L^2(e)} = \int_e \psi_e L(v_e)\hat J_e[(\boldsymbol\sigma_h-\nabla u_h)\cdot\mathbf t_T]. \tag{4.29}$$

Now, integrating by parts on each triangle $T\subseteq w_e$, noting that $\mathrm{curl}(\boldsymbol\sigma_h-\nabla u_h)=0$ in Ω, and employing Cauchy–Schwarz's inequality, we find that

$$\int_e \psi_e L(v_e)\hat J_e[(\boldsymbol\sigma_h-\nabla u_h)\cdot\mathbf t_T] = \int_{w_e} \mathbf{curl}(\psi_e L(v_e))\cdot(\boldsymbol\sigma_h-\nabla u_h)$$
$$\leqslant \|\mathbf{curl}(\psi_e L(v_e))\|_{[L^2(w_e)]^2}\|\boldsymbol\sigma_h-\nabla u_h\|_{[L^2(w_e)]^2}. \tag{4.30}$$

On the other hand, applying the local inverse inequality to the polynomial $\psi_e L(v_e)$ (see [11, Theorem 3.2.6]), and using the estimate (4.21), and the fact that $0\leqslant\psi_e^{1/2}\leqslant 1$, we deduce that

$$\|\mathbf{curl}(\psi_e L(v_e))\|_{[L^2(w_e)]^2} = |\psi_e L(v_e)|_{H^1(w_e)} \leqslant c h_e^{-1}\|\psi_e L(v_e)\|_{L^2(w_e)}$$
$$\leqslant c h_e^{-1/2}\|\psi_e^{1/2}L(v_e)\|_{L^2(e)} \leqslant c h_e^{-1/2}\|v_e\|_{L^2(e)}. \tag{4.31}$$

Finally, (4.28) follows from (4.29)–(4.31). □

As a direct consequence of Lemma 4.6, noting that the number of triangles of each w_e is at most 2, and adding and subtracting $\boldsymbol\sigma=\nabla u$ on the right-hand side of (4.28), we deduce now that there exists $C>0$, independent of h and $\tilde h$, such that

$$\sum_{e\in E_h(\Omega)} h_e\|J[(\boldsymbol{\sigma}_h-\nabla u_h)\cdot \mathbf{t}_T]\|^2_{L^2(e)}\leqslant C\{\|\boldsymbol{\sigma}-\boldsymbol{\sigma}_h\|^2_{[L^2(\Omega)]^2}+|u-u_h|^2_{H^1(\Omega)}\},\tag{4.32}$$

and

$$\sum_{e\in E_h(\Gamma)} h_e\|(\boldsymbol{\sigma}_h-\nabla u_h)\cdot \mathbf{t}_T\|^2_{L^2(e)}\leqslant C\{\|\boldsymbol{\sigma}-\boldsymbol{\sigma}_h\|^2_{[L^2(\Omega)]^2}+|u-u_h|^2_{H^1(\Omega)}\}.\tag{4.33}$$

In order to bound the last term in (4.2) we recall the following result from [17].

Lemma 4.7. *There exists* $c>0$, *independent of* h *and* $\tilde{h}$, *such that*

$$\log[1+C_{\tilde{h}}(\Gamma_{\mathrm{N}})]\sum_{e\in E_h(\Gamma_{\mathrm{N}})}\tilde{h}_e\|g-\boldsymbol{\sigma}_h\cdot\boldsymbol{v}\|^2_{L^2(e)}\leqslant c\{\|\boldsymbol{\sigma}-\boldsymbol{\sigma}_h\|^2_{[L^2(\Omega)]^2}+h^2\|\mathrm{div}(\boldsymbol{\sigma}-\boldsymbol{\sigma}_h)\|^2_{L^2(\Omega)}\}.$$

Proof. See [17, Lemma 5.9, Eq. (5.25)]. □

It follows easily from the previous lemma that

$$\log[1+C_{\tilde{h}}(\Gamma_{\mathrm{N}})]\sum_{e\in E_h(\Gamma_{\mathrm{N}})}\tilde{h}_e\|g-\boldsymbol{\sigma}_h\cdot\boldsymbol{v}\|^2_{L^2(e)}\leqslant C\|\boldsymbol{\sigma}-\boldsymbol{\sigma}_h\|^2_{H(\mathrm{div};\Omega)}.\tag{4.34}$$

Finally, the efficiency estimate of the a posteriori error estimate is a straightforward consequence of (4.22)–(4.24), (4.32)–(4.34).

5. A Ritz projection-based a posteriori error analysis

In this section, we introduce and analyze a second reliable a posteriori error estimate for our boundary value problem. To this end, we now define the Ritz projection of the error with respect to the inner product of $\mathbf{H}$, as the unique $(\bar{\boldsymbol{\sigma}},\bar{u})\in\mathbf{H}$ such that

$$\langle(\bar{\boldsymbol{\sigma}},\bar{u}),(\boldsymbol{\tau},v)\rangle_{\mathbf{H}}=A((\boldsymbol{\sigma}-\boldsymbol{\sigma}_h,u-u_h),(\boldsymbol{\tau},v))+B((\boldsymbol{\tau},v),\xi-\xi_{\tilde{h}})\quad\forall(\boldsymbol{\tau},v)\in\mathbf{H},\tag{5.1}$$

where $\langle(\bar{\boldsymbol{\sigma}},\bar{u}),(\boldsymbol{\tau},v)\rangle_{\mathbf{H}}:=\langle\bar{\boldsymbol{\sigma}},\boldsymbol{\tau}\rangle_{H(\mathrm{div};\Omega)}+\langle\bar{u},v\rangle_{H^1(\Omega)}$, and $\langle\cdot,\cdot\rangle_{H(\mathrm{div};\Omega)}$ and $\langle\cdot,\cdot\rangle_{H^1(\Omega)}$ denote the usual inner products of $H(\mathrm{div};\Omega)$ and $H^1(\Omega)$, respectively. The existence and uniqueness of $(\bar{\boldsymbol{\sigma}},\bar{u})$ is guaranteed by the fact that the right-hand side of (5.1) is a linear and bounded functional on $\mathbf{H}$. The following lemma provides an upper bound for $\|(\bar{\boldsymbol{\sigma}},\bar{u})\|_{\mathbf{H}}$.

Lemma 5.1. *There exists* $C>0$, *independent of* h *and* $\tilde{h}$, *such that*

$$\|(\bar{\boldsymbol{\sigma}},\bar{u})\|^2_{\mathbf{H}}\leqslant C\{\|f+\mathrm{div}\,\boldsymbol{\sigma}_h\|^2_{L^2(\Omega)}+\|\boldsymbol{\sigma}_h-\nabla u_h\|^2_{[L^2(\Omega)]^2}+\|u_h+\xi_{\tilde{h}}\|^2_{H^{1/2}_{00}(\Gamma_{\mathrm{N}})}\}.\tag{5.2}$$

Proof. We see from the first equation in (2.5) that

$$A((\boldsymbol{\sigma},u),(\boldsymbol{\tau},v))+B((\boldsymbol{\tau},v),\xi)=F(\boldsymbol{\tau},v),$$

and thus (5.1) reduces to

$$\langle(\bar{\boldsymbol{\sigma}},\bar{u}),(\boldsymbol{\tau},v)\rangle_{\mathbf{H}}=F(\boldsymbol{\tau},v)-A((\boldsymbol{\sigma}_h,u_h),(\boldsymbol{\tau},v))-B((\boldsymbol{\tau},v),\xi_{\tilde{h}})\quad\forall(\boldsymbol{\tau},v)\in\mathbf{H}.\tag{5.3}$$

It follows, according to the definitions of A, B, and F (cf. (2.6)–(2.8)), that (5.3) is equivalent to

$$\langle\bar{\boldsymbol{\sigma}},\boldsymbol{\tau}\rangle_{H(\mathrm{div};\Omega)}=F_1(\boldsymbol{\tau})\quad\forall\boldsymbol{\tau}\in H(\mathrm{div};\Omega),\tag{5.4}$$

and

$$\langle \bar{u}, v\rangle_{H^1(\Omega)} = F_2(v) \quad \forall v \in H^1_{\Gamma_{\mathrm{D}}}(\Omega), \tag{5.5}$$

where F_1 and F_2 are the linear and bounded functionals defined by

$$F_1(\boldsymbol{\tau}) := -\int_\Omega (f + \operatorname{div}\boldsymbol{\sigma}_h)\operatorname{div}\boldsymbol{\tau} - \int_\Omega \boldsymbol{\sigma}_h\cdot\boldsymbol{\tau} - \int_\Omega u_h \operatorname{div}\boldsymbol{\tau} - \frac{1}{2}\int_\Omega (\nabla u_h - \boldsymbol{\sigma}_h)\cdot\boldsymbol{\tau} - \langle \boldsymbol{\tau}\cdot\boldsymbol{v}, \xi_{\tilde{h}}\rangle_{\Gamma_{\mathrm{N}}}, \tag{5.6}$$

and

$$F_2(v) := \int_\Omega (f + \operatorname{div}\boldsymbol{\sigma}_h)v - \frac{1}{2}\int_\Omega (\nabla u_h - \boldsymbol{\sigma}_h)\cdot\nabla v. \tag{5.7}$$

In addition, integrating by parts $\int_\Omega u_h \operatorname{div}\boldsymbol{\tau}$, we observe that F_1 simplifies to

$$F_1(\boldsymbol{\tau}) := -\int_\Omega (f + \operatorname{div}\boldsymbol{\sigma}_h)\operatorname{div}\boldsymbol{\tau} - \frac{1}{2}\int_\Omega (\boldsymbol{\sigma}_h - \nabla u_h)\cdot\boldsymbol{\tau} - \langle \boldsymbol{\tau}\cdot\boldsymbol{v}, u_h + \xi_{\tilde{h}}\rangle_{\Gamma_{\mathrm{N}}}. \tag{5.8}$$

Finally, it is clear from the formulations (5.4) and (5.5) that $\|\bar{\boldsymbol{\sigma}}\|_{H(\mathrm{div};\Omega)} = \|F_1\|_{(H(\mathrm{div};\Omega))'}$ and $\|\bar{u}\|_{H^1(\Omega)} = \|F_2\|_{(H^1_{\Gamma_{\mathrm{D}}}(\Omega))'}$, whence (5.8) and (5.7) yield, respectively,

$$\|\bar{\boldsymbol{\sigma}}\|^2_{H(\mathrm{div};\Omega)} \leqslant c\{\|f + \operatorname{div}\boldsymbol{\sigma}_h\|^2_{L^2(\Omega)} + \|\boldsymbol{\sigma}_h - \nabla u_h\|^2_{[L^2(\Omega)]^2} + \|u_h + \xi_{\tilde{h}}\|^2_{H^{1/2}_{00}(\Gamma_{\mathrm{N}})}\},$$

and

$$\|\bar{u}\|^2_{H^1(\Omega)} \leqslant c\{\|f + \operatorname{div}\boldsymbol{\sigma}_h\|^2_{L^2(\Omega)} + \|\boldsymbol{\sigma}_h - \nabla u_h\|^2_{[L^2(\Omega)]^2}\}.$$

This provides the required estimate and completes the proof. □

The following theorem establishes a reliable and efficient *quasi-local* a posteriori error estimate $\tilde{\boldsymbol{\theta}}$ for our augmented mixed finite element scheme. It makes use of the continuous dependence result given by (2.10) (cf. Theorem 2.1), the Ritz projection $(\bar{\boldsymbol{\sigma}}, \bar{u})$, and the associated upper bound provided by Lemma 5.1. The name *quasi-local* refers to the fact that one of the terms defining $\tilde{\boldsymbol{\theta}}$ can not be decomposed into local quantities associated to each triangle $T \in \mathscr{T}_h$ (unless it is either conveniently bounded or previously modified, as we will see below).

Theorem 5.1. *Let* $((\boldsymbol{\sigma}, u), \xi) \in \mathbf{H} \times Q$ *and* $((\boldsymbol{\sigma}_h, u_h), \xi_{\tilde{h}}) \in \mathbf{H}_h \times Q_{\tilde{h}}$ *be the unique solutions of the continuous and discrete formulations* (2.5) *and* (3.5), *respectively. Then, there exist positive constants* $\tilde{C}_{\mathrm{eff}}, \tilde{C}_{\mathrm{rel}}$, *independent of h and* $\tilde{h}$, *such that*

$$\tilde{C}_{\mathrm{eff}}\tilde{\boldsymbol{\theta}}^2 \leqslant \|((\boldsymbol{\sigma} - \boldsymbol{\sigma}_h, u - u_h), \xi - \xi_{\tilde{h}})\|^2_{\mathbf{H}\times Q} \leqslant \tilde{C}_{\mathrm{rel}}\tilde{\boldsymbol{\theta}}^2, \tag{5.9}$$

where $\tilde{\boldsymbol{\theta}}^2 := \sum_{T\in\mathscr{T}_h}\tilde{\theta}_T^2 + \|u_h + \xi_{\tilde{h}}\|^2_{H^{1/2}_{00}(\Gamma_{\mathrm{N}})}$, *and for each* $T \in \mathscr{T}_h$ *we define*

$$\tilde{\theta}_T^2 := \|f + \operatorname{div}\boldsymbol{\sigma}_h\|^2_{L^2(T)} + \|\boldsymbol{\sigma}_h - \nabla u_h\|^2_{[L^2(T)]^2} + \log[1 + C_{\tilde{h}}(\Gamma_{\mathrm{N}})] \sum_{e\in E(T)\cap E_h(\Gamma_{\mathrm{N}})} \tilde{h}_e\|g - \boldsymbol{\sigma}_h\cdot\boldsymbol{v}\|^2_{L^2(e)}.$$

Proof. It is not difficult to see that the first inequality in the continuous dependence result given by (2.10) constitutes a global inf–sup condition for the linear operator arising after adding the two equations of the variational formulation (2.5). Then, applying this estimate to the error $((\boldsymbol{\sigma} - \boldsymbol{\sigma}_h, u - u_h), \xi - \xi_{\tilde{h}}) \in \mathbf{H}$, and using the definition of the Ritz projection (cf. (5.1)), we find that

$$\begin{aligned}
&\|((\boldsymbol{\sigma}-\boldsymbol{\sigma}_h, u-u_h), \xi-\xi_{\tilde{h}})\|_{\mathbf{H}\times Q} \\
&\leqslant C \sup_{\substack{((\boldsymbol{\tau},v),\lambda)\in\mathbf{H}\times Q\\((\boldsymbol{\tau},v),\lambda)\neq 0}} \frac{A((\boldsymbol{\sigma}-\boldsymbol{\sigma}_h, u-u_h),(\boldsymbol{\tau},v)) + B((\boldsymbol{\tau},v),\xi-\xi_{\tilde{h}}) + B((\boldsymbol{\sigma}-\boldsymbol{\sigma}_h,u-u_h),\lambda)}{\|((\boldsymbol{\tau},v),\lambda)\|_{\mathbf{H}\times Q}} \\
&= C \sup_{\substack{((\boldsymbol{\tau},v),\lambda)\in\mathbf{H}\times Q\\((\boldsymbol{\tau},v),\lambda)\neq 0}} \frac{\langle(\bar{\boldsymbol{\sigma}},\bar{u}),(\boldsymbol{\tau},v)\rangle_{\mathbf{H}} + \langle g-\boldsymbol{\sigma}_h\cdot\boldsymbol{v},\lambda\rangle_{\Gamma_{\mathrm{N}}}}{\|((\boldsymbol{\tau},v),\lambda)\|_{\mathbf{H}\times Q}},
\end{aligned}$$

which yields

$$\|((\boldsymbol{\sigma}-\boldsymbol{\sigma}_h, u-u_h), \xi-\xi_{\tilde{h}})\|^2_{\mathbf{H}\times Q} \leqslant C\{\|(\bar{\boldsymbol{\sigma}},\bar{u})\|^2_{\mathbf{H}} + \|g-\boldsymbol{\sigma}_h\cdot\boldsymbol{v}\|^2_{H^{-1/2}(\Gamma_{\mathrm{N}})}\}. \tag{5.10}$$

In this way, the reliability of $\tilde{\boldsymbol{\theta}}$, which is given by the right-hand side of (5.9), follows from the upper bound (5.2) for the Ritz projection, together with the estimates (4.15) and (4.16) bounding the Neumann residual.

Now, for the efficiency of $\tilde{\boldsymbol{\theta}}$ we proceed as follows. The terms defining $\tilde{\theta}_T^2$ are bounded as in (4.22), (4.23), and (4.34) which gives

$$\sum_{T\in\mathcal{T}} \tilde{\theta}_T^2 \leqslant C\{|u-u_h|^2_{H^1(\Omega)} + \|\boldsymbol{\sigma}-\boldsymbol{\sigma}_h\|^2_{H(\mathrm{div};\Omega)}\}, \tag{5.11}$$

whereas for the second term defining $\tilde{\boldsymbol{\theta}}^2$ we add and subtract $\xi = -u|_{\Gamma_{\mathrm{N}}}$, and then apply the trace theorem, to obtain:

$$\|u_h+\xi_{\tilde{h}}\|^2_{H^{1/2}_{00}(\Gamma_{\mathrm{N}})} \leqslant C\left\{\|u-u_h\|^2_{H^1(\Omega)} + \|\xi-\xi_{\tilde{h}}\|^2_{H^{1/2}_{00}(\Gamma_{\mathrm{N}})}\right\}. \tag{5.12}$$

In this way, (5.11) and (5.12) imply the left-hand side of (5.9) and finish the proof. □

At this point we remark that the eventual use of $\tilde{\boldsymbol{\theta}}$ in an adaptive algorithm solving (3.5) would be discouraged by the non-local character of the expression $\|u_h+\xi_{\tilde{h}}\|^2_{H^{1/2}_{00}(\Gamma_{\mathrm{N}})}$. In order to circumvent this, as mentioned before, we now apply an interpolation argument and replace this term by a suitable upper bound, which yields a reliable and fully local a posteriori error estimate.

Theorem 5.2. *There exists a positive constant $\hat{C}_{\mathrm{rel}}$, independent of h and $\tilde{h}$, such that*

$$\|((\boldsymbol{\sigma}-\boldsymbol{\sigma}_h, u-u_h), \xi-\xi_{\tilde{h}})\|^2_{\mathbf{H}\times Q} \leqslant \hat{C}_{\mathrm{rel}}\hat{\boldsymbol{\theta}}^2, \tag{5.13}$$

where $\hat{\boldsymbol{\theta}}^2 := \sum_{T\in\mathcal{T}_h}\hat{\theta}_T^2$, and for each $T\in\mathcal{T}_h$ we define

$$\begin{aligned}
\hat{\theta}_T^2 := {} & \|f+\operatorname{div}\boldsymbol{\sigma}_h\|^2_{L^2(T)} + \|\boldsymbol{\sigma}_h-\nabla u_h\|^2_{[L^2(T)]^2} + \sum_{e\in E(T)\cap E_h(\Gamma_{\mathrm{N}})} \|u_h+\xi_{\tilde{h}}\|^2_{H^1(e)} \\
& + \log[1+C_{\tilde{h}}(\Gamma_{\mathrm{N}})] \sum_{e\in E(T)\cap E_h(\Gamma_{\mathrm{N}})} \tilde{h}_e\|g-\boldsymbol{\sigma}_h\cdot\boldsymbol{v}\|^2_{L^2(e)}.
\end{aligned}$$

Proof. Since $H^{1/2}_{00}(\Gamma_{\mathrm{N}})$ is the interpolation space with index $\frac{1}{2}$ between $H^1_0(\Gamma_{\mathrm{N}})$ and $L^2(\Gamma_{\mathrm{N}})$, there holds

$$\begin{aligned}
\|u_h+\xi_{\tilde{h}}\|^2_{H^{1/2}_{00}(\Gamma_{\mathrm{N}})} &\leqslant C\{\|u_h+\xi_{\tilde{h}}\|_{L^2(\Gamma_{\mathrm{N}})}|u_h+\xi_{\tilde{h}}|_{H^1(\Gamma_{\mathrm{N}})}\} \\
&\leqslant C\|u_h+\xi_{\tilde{h}}\|^2_{H^1(\Gamma_{\mathrm{N}})} = C\sum_{e\in E_h(\Gamma_{\mathrm{N}})}\|u_h+\xi_{\tilde{h}}\|^2_{H^1(e)}.
\end{aligned}$$

This estimate and the upper bound in (5.9) provide (5.13) and complete the proof. □

On the other hand, we now deal differently with the original expression of the functional F_1 in (5.6) and derive an alternative upper bound for the Ritz projection, which can be entirely decomposed into local terms. More precisely, we have the following result.

Lemma 5.2. *Let $\bar{u}_h$ be the unique function in a Lagrange finite element subspace X_h of $H^1_{\Gamma_{\mathrm{D}}}(\Omega)$ such that $\bar{u}_h(\mathbf{x})=u_h(\mathbf{x})$ for each node $\mathbf{x}\in\Omega\cup\Gamma_{\mathrm{D}}$, and $\bar{u}_h(\mathbf{x})=-\xi_{\tilde{h}}(\mathbf{x})$ for each node $\mathbf{x}\in\Gamma_{\mathrm{N}}$. Then, there exists $C>0$, independent of h and $\tilde{h}$, such that*

$$\begin{aligned}\|(\bar{\boldsymbol{\sigma}},\bar{u})\|^2_{\mathbf{H}}\leqslant C\Big\{&\|f+\operatorname{div}\boldsymbol{\sigma}_h\|^2_{L^2(\Omega)}+\|\boldsymbol{\sigma}_h-\nabla u_h\|^2_{[L^2(\Omega)]^2}\\&+\|\boldsymbol{\sigma}_h-\nabla\bar{u}_h\|^2_{[L^2(\Omega)]^2}+\|u_h-\bar{u}_h\|^2_{L^2(\Omega)}+\|\bar{u}_h+\xi_{\tilde{h}}\|^2_{H^{1/2}_{00}(\Gamma_{\mathrm{N}})}\Big\}.\end{aligned}\tag{5.14}$$

Proof. Adding and subtracting $\bar{u}_h$ in the term $\int_\Omega u_h\operatorname{div}\boldsymbol{\tau}$ appearing in the definition of the functional F_1 (cf. (5.6)), and then integrating by parts $\int_\Omega\bar{u}_h\operatorname{div}\boldsymbol{\tau}$, gives

$$\begin{aligned}F_1(\boldsymbol{\tau}):=&-\int_\Omega(f+\operatorname{div}\boldsymbol{\sigma}_h)\operatorname{div}\boldsymbol{\tau}+\int_\Omega(\nabla\bar{u}_h-\boldsymbol{\sigma}_h)\cdot\boldsymbol{\tau}-\int_\Omega(u_h-\bar{u}_h)\operatorname{div}\boldsymbol{\tau}\\&-\frac{1}{2}\int_\Omega(\nabla u_h-\boldsymbol{\sigma}_h)\cdot\boldsymbol{\tau}-\langle\boldsymbol{\tau}\cdot\boldsymbol{\nu},\bar{u}_h+\xi_{\tilde{h}}\rangle_{\Gamma_{\mathrm{N}}}\quad\forall\boldsymbol{\tau}\in H(\operatorname{div};\Omega).\end{aligned}$$

The rest of the proof proceeds as in Lemma 5.1 bounding now $\|F_1\|_{H(\operatorname{div};\Omega)'}$ from the above expression. We omit further details. □

At first glance, the new upper bound (5.14) looks more complicated than (5.2) and yet it does not get rid, apparently, of the non-local term $\|\bar{u}_h+\xi_{\tilde{h}}\|^2_{H^{1/2}_{00}(\Gamma_{\mathrm{N}})}$. Nevertheless, the fact that the function $\bar{u}_h+\xi_{\tilde{h}}$ now vanishes at the nodes of Γ_{N} (which was not necessarily the case with u_h) allows us to estimate its $H^{1/2}_{00}(\Gamma_{\mathrm{N}})$-norm in terms of L^2-local norms on the edges of Γ_{N}. More precisely, according to Theorem 1 in [9], there holds

$$\|\bar{u}_h+\xi_{\tilde{h}}\|^2_{H^{1/2}_{00}(\Gamma_{\mathrm{N}})}\leqslant C\,\log[1+C_h(\Gamma_{\mathrm{N}})]\sum_{e\in E_h(\Gamma_{\mathrm{N}})}h_e\left\|\frac{\mathrm{d}\bar{u}_h}{\mathrm{d}\mathbf{t}_T}+\frac{\mathrm{d}\xi_{\tilde{h}}}{\mathrm{d}\mathbf{t}_T}\right\|^2_{L^2(e)},\tag{5.15}$$

where $C_h(\Gamma_{\mathrm{N}}):=\max\{|\Gamma_i|/|\Gamma_j|:\ |i-j|=1,i,j\in\{1,\ldots,n\}\}$ and $\{\Gamma_1,\Gamma_2,\ldots,\Gamma_n\}$ is the partition on Γ_{N} induced by $\mathscr{T}_h$.

In addition, in the particular case in which the finite element subspace X_h is given by (3.4), we easily deduce that $\bar{u}_h+\xi_{\tilde{h}}$ vanishes identically on Γ_{N}. Indeed, since each edge Γ_i is contained in an edge $\tilde{\Gamma}_j$ and the end points of each $\tilde{\Gamma}_j$ are nodes of $\mathscr{T}_h$, the above statement follows from the fact that $Q_{\tilde{h}}$ (cf. (3.2)) is also piecewise linear on the independent partition $\{\tilde{\Gamma}_1,\ldots,\tilde{\Gamma}_m\}$ of Γ_{N}.

On the other hand, since $u_h=\bar{u}_h$ on each $T\in\mathscr{T}_h$ not touching the Neumann boundary Γ_{N}, we see that $\|u_h-\bar{u}_h\|_{L^2(T)}$ vanishes and $\|\boldsymbol{\sigma}_h-\nabla\bar{u}_h\|^2_{[L^2(T)]^2}$ becomes $\|\boldsymbol{\sigma}_h-\nabla u_h\|^2_{[L^2(T)]^2}$ on these triangles. This property of the auxiliary function $\bar{u}_h$ induces the definition of the following parameter associated to each $T\in\mathscr{T}_h$:

$$\kappa(T):=\begin{cases}1&\text{if }\partial T\cap\bar{\Gamma}_{\mathrm{N}}\neq\phi,\\0&\text{otherwise.}\end{cases}\tag{5.16}$$

Consequently, we are now in a position to establish a reliable and *quasi-efficient* fully local a posteriori error estimate. Here, the *quasi-efficiency* refers to the extra term appearing below on the right-hand side of (5.18).

Theorem 5.3. *There exist positive constants C_{rel}, C_{eff}, independent of h and $\tilde{h}$, such that*

$$\|((\boldsymbol{\sigma}-\boldsymbol{\sigma}_h,u-u_h),\xi-\xi_{\tilde{h}})\|^2_{\mathbf{H}\times Q}\leqslant C_{\mathrm{rel}}\,\boldsymbol{\theta}^2,\tag{5.17}$$

and

$$C_{\mathrm{eff}}\boldsymbol{\theta}^2 \leqslant \|((\boldsymbol{\sigma}-\boldsymbol{\sigma}_h, u-u_h), \xi-\xi_{\tilde{h}})\|^2_{\mathbf{H}\times Q} + \sum_{T\in\mathscr{T}_h} \kappa(T)\|u-\bar{u}_h\|^2_{H^1(T)}, \tag{5.18}$$

where $\boldsymbol{\theta}^2 := \sum_{T\in\mathscr{T}_h}\theta_T^2$, *and for each* $T\in\mathscr{T}_h$ *we define*

$$\begin{aligned}\theta_T^2 := {} & \|f+\operatorname{div}\boldsymbol{\sigma}_h\|^2_{L^2(T)} + \|\boldsymbol{\sigma}_h-\nabla u_h\|^2_{[L^2(T)]^2} + \kappa(T)\|\boldsymbol{\sigma}_h-\nabla\bar{u}_h\|^2_{[L^2(T)]^2}\\ & + \kappa(T)\|u_h-\bar{u}_h\|^2_{L^2(T)} + \log[1+C_{\tilde{h}}(\Gamma_{\mathrm{N}})] \sum_{e\in E(T)\cap E_h(\Gamma_{\mathrm{N}})} \tilde{h}_e\|g-\boldsymbol{\sigma}_h\cdot\boldsymbol{v}\|^2_{L^2(e)}\\ & + \log[1+C_h(\Gamma_{\mathrm{N}})] \sum_{e\in E(T)\cap E_h(\Gamma_{\mathrm{N}})} h_e \left\|\frac{\mathrm{d}\bar{u}_h}{\mathrm{d}\mathbf{t}_T}+\frac{\mathrm{d}\xi_{\tilde{h}}}{\mathrm{d}\mathbf{t}_T}\right\|^2_{L^2(e)}.\end{aligned}$$

In particular, if the finite element subspace X_h *is given by* (3.4), θ_T^2 *simplifies to*

$$\begin{aligned}\theta_T^2 := {} & \|f+\operatorname{div}\boldsymbol{\sigma}_h\|^2_{L^2(T)} + \|\boldsymbol{\sigma}_h-\nabla u_h\|^2_{[L^2(T)]^2} + \kappa(T)\|\boldsymbol{\sigma}_h-\nabla\bar{u}_h\|^2_{[L^2(T)]^2}\\ & + \kappa(T)\|u_h-\bar{u}_h\|^2_{L^2(T)} + \log[1+C_{\tilde{h}}(\Gamma_{\mathrm{N}})] \sum_{e\in E(T)\cap E_h(\Gamma_{\mathrm{N}})} \tilde{h}_e\|g-\boldsymbol{\sigma}_h\cdot\boldsymbol{v}\|^2_{L^2(e)}.\end{aligned} \tag{5.19}$$

Proof. The reliability of $\boldsymbol{\theta}$ follows easily from (5.10), the estimate for the Neumann residual given by (4.15) and (4.16), the upper bound for the Ritz projection provided by Lemma 5.2, and the previous analysis yielding (5.15) and (5.16).

On the other hand, for the quasi-efficiency we first observe, after adding and subtracting $\boldsymbol{\sigma}=\nabla u$ in the second and third term defining $\boldsymbol{\theta}_T$, and u in the fourth one, that

$$\begin{aligned}& \|f+\operatorname{div}\boldsymbol{\sigma}_h\|^2_{L^2(T)} + \|\boldsymbol{\sigma}_h-\nabla u_h\|^2_{[L^2(T)]^2} + \kappa(T)\|\boldsymbol{\sigma}_h-\nabla\bar{u}_h\|^2_{[L^2(T)]^2} + \kappa(T)\|u_h-\bar{u}_h\|^2_{L^2(T)}\\ & \quad \leqslant C\left\{\|\boldsymbol{\sigma}-\boldsymbol{\sigma}_h\|^2_{H(\mathrm{div};T)} + \|u-u_h\|^2_{H^1(T)} + \kappa(T)\|u-\bar{u}_h\|^2_{H^1(T)}\right\}.\end{aligned} \tag{5.20}$$

Next, we know from (4.34) that

$$\log[1+C_{\tilde{h}}(\Gamma_{\mathrm{N}})] \sum_{e\in E_h(\Gamma_{\mathrm{N}})} \tilde{h}_e\|g-\boldsymbol{\sigma}_h\cdot\boldsymbol{v}\|^2_{L^2(e)} \leqslant C\|\boldsymbol{\sigma}-\boldsymbol{\sigma}_h\|^2_{H(\mathrm{div};\Omega)}, \tag{5.21}$$

and applying the same arguments of Lemma 4.5 we find that

$$\log[1+C_h(\Gamma_{\mathrm{N}})] \sum_{e\in E_h(\Gamma_{\mathrm{N}})} h_e \left\|\frac{\mathrm{d}\bar{u}_h}{\mathrm{d}\mathbf{t}_T}+\frac{\mathrm{d}\xi_{\tilde{h}}}{\mathrm{d}\mathbf{t}_T}\right\|^2_{L^2(e)} \leqslant C\{\|\xi-\xi_{\tilde{h}}\|^2_{H^{1/2}_{00}(\Gamma_{\mathrm{N}})} + \|u-\bar{u}_h\|^2_{H^1(\Omega)}\}. \tag{5.22}$$

In this way, (5.18) is a straightforward consequence of (5.20)–(5.22). □

6. Numerical results

In this section, we present several examples illustrating the performance of the augmented mixed finite element method (3.5) and the associated adaptive algorithms using the a posteriori error estimates $\boldsymbol{\eta}$ and $\boldsymbol{\theta}$ (cf. Theorems 4.1 and 5.3). All the numerical results given below were obtained in a *Compaq Alpha ES40 Parallel Computer* using a Fortran 90 code. The nonsymmetric (3.5) is solved by using a LU factorization method for sparse matrices. In addition, the errors on each triangle are calculated using a seven points quadrature rule (see [23, p. 314]).

We begin with some further notations. In what follows, N denotes the number of degrees of freedom defining the subspaces $\mathbf{H}_h$ and $Q_{\tilde{h}}$, that is $N :=$ number of edges of $\mathscr{T}_h$ + number of nodes in $(\bar{\Omega}-\bar{\Gamma}_{\mathrm{D}})+(m-1)$. We recall

Table 1
Individual errors, total errors, and experimental rates of convergence for a sequence of uniform refinements (Example 1)

h	$\mathbf{e}_0(u)$	$\mathbf{r}_0(u)$	$\mathbf{e}_1(u)$	$\mathbf{r}_1(u)$	$\mathbf{e}(u)$	$\mathbf{r}(u)$
0.5190E + 0	0.5623E − 1	—	0.2081E + 0	—	0.2155E + 0	—
0.2595E + 0	0.1321E − 1	2.0897	0.7601E − 1	1.4530	0.7714E − 1	1.4821
0.1297E + 0	0.3191E − 2	2.0484	0.3312E − 1	1.1978	0.3327E − 1	1.2125
0.6488E − 1	0.7880E − 3	2.0190	0.1581E − 1	1.0675	0.1583E − 1	1.0722
0.3244E − 1	0.1961E − 3	2.0066	0.7801E − 2	1.0191	0.7803E − 2	1.0205
0.1622E − 1	0.4897E − 4	2.0016	0.3885E − 2	1.0057	0.3885E − 2	1.0061
0.8110E − 2	0.1252E − 4	1.9676	0.1941E − 2	1.0011	0.1940E − 2	1.0018
h	$\mathbf{e}(\boldsymbol{\sigma})$	$\mathbf{r}(\boldsymbol{\sigma})$	$\mathbf{e}(\xi)$	$\mathbf{r}(\xi)$	$\mathbf{e}$	$\mathbf{r}(\mathbf{e})$
0.5190E + 0	0.2519E + 0	—	0.2834E + 0	—	0.4362E + 0	—
0.2595E + 0	0.9847E − 1	1.3550	0.9987E − 1	1.5047	0.1601E + 0	1.4460
0.1297E + 0	0.4490E − 1	1.1323	0.4108E − 1	1.2809	0.6936E − 1	1.2061
0.6488E − 1	0.2178E − 1	1.0444	0.1859E − 1	1.1446	0.3273E − 1	1.0842
0.3244E − 1	0.1079E − 1	1.0133	0.8786E − 2	1.0812	0.1595E − 1	1.0370
0.1622E − 1	0.5386E − 2	1.0024	0.4234E − 2	1.0531	0.7876E − 2	1.0180
0.8110E − 2	0.2691E − 2	1.0010	0.2081E − 2	1.0247	0.3916E − 2	1.0080

here that $\{\tilde{\Gamma}_1, \tilde{\Gamma}_2, \ldots, \tilde{\Gamma}_m\}$ is the independent partition of Γ_{N}, and, according to the stability condition required in Theorem 3.1, we now set a vertex of it every two vertices of the partition on Γ_{N} inherited from $\mathscr{T}_h$.

On the other hand, the individual and total errors are defined by

$$\mathbf{e}(\boldsymbol{\sigma}) := \|\boldsymbol{\sigma} - \boldsymbol{\sigma}_h\|_{H(\mathrm{div};\Omega)}, \quad \mathbf{e}_0(u) := \|u - u_h\|_{L^2(\Omega)}, \quad \mathbf{e}_1(u) := |u - u_h|_{H^1(\Omega)},$$

$$\mathbf{e}(u) := \|u - u_h\|_{H^1(\Omega)}, \quad \mathbf{e}(\xi) := \|\xi - \xi_{\tilde{h}}\|_{H_{00}^{1/2}(\Gamma_{\mathrm{N}})},$$

and

$$\mathbf{e} := \{[\mathbf{e}(\boldsymbol{\sigma})]^2 + [\mathbf{e}(u)]^2 + [\mathbf{e}(\xi)]^2\}^{1/2},$$

where $((\boldsymbol{\sigma}, u), \xi) \in \mathbf{H} \times Q$ and $((\boldsymbol{\sigma}_h, u_h), \xi_{\tilde{h}}) \in \mathbf{H}_h \times Q_{\tilde{h}}$ are the unique solutions of (2.5) and (3.5), respectively. In addition, we introduce the experimental rates of convergence

$$\mathbf{r}(\boldsymbol{\sigma}) := \frac{\log(\mathbf{e}(\boldsymbol{\sigma})/\mathbf{e}'(\boldsymbol{\sigma}))}{\log(h/h')}, \quad \mathbf{r}_0(u) := \frac{\log(\mathbf{e}_0(u)/\mathbf{e}'_0(u))}{\log(h/h')}, \quad \mathbf{r}_1(u) := \frac{\log(\mathbf{e}_1(u)/\mathbf{e}'_1(u))}{\log(h/h')}.$$

$$\mathbf{r}(u) := \frac{\log(\mathbf{e}(u)/\mathbf{e}'(u))}{\log(h/h')}, \quad \mathbf{r}(\xi) := \frac{\log(\mathbf{e}(\xi)/\mathbf{e}'(\xi))}{\log(h/h')}, \quad \text{and} \quad \mathbf{r}(\mathbf{e}) := \frac{\log(\mathbf{e}/\mathbf{e}')}{\log(h/h')},$$

where $\mathbf{e}(\cdot)$ and $\mathbf{e}'(\cdot)$ (resp. $\mathbf{e}$ and $\mathbf{e}'$ or $\mathbf{e}_j(u)$ and $\mathbf{e}'_j(u)$, $j \in \{0, 1\}$) denote the corresponding errors at two consecutive triangulations with mesh sizes h and h', respectively.

We first illustrate the performance of our augmented mixed finite element method (3.5) when a uniform refinement is employed. To this end, we consider three examples of boundary value problems with smooth solutions on the square $\Omega :=]0, 1[^2$ with $\Gamma_{\mathrm{D}} := [0, 1] \times \{0\} \cup \{0\} \times [0, 1]$ and $\Gamma_{\mathrm{N}} := \Gamma - \bar{\Gamma}_{\mathrm{D}}$. We chose the data f and g so that the exact solutions are given by

$$u(\mathbf{x}) := \sin(x_1)\sin(x_2), \quad u(\mathbf{x}) := x_1 x_2 \sin(x_1^2 + x_2^2), \quad \text{and} \quad u(\mathbf{x}) := \frac{x_1^2 x_2^2}{x_1^2 + x_2^2 + 5}$$

for each $\mathbf{x} := (x_1, x_2) \in \Omega$, in the Examples 1–3, respectively. In Tables 1–3 we provide the individual errors, the total error, and the experimental rates of convergence on a sequence of uniform meshes. Given a coarse uniform initial triangulation, each subsequent mesh is obtained from the previous one by dividing each triangle into the four ones arising when connecting the midpoints of its sides. We observe that the rate of convergence $\mathrm{O}(h)$ predicted by

Table 2
Individual errors, total errors, and experimental rates of convergence for a sequence of uniform refinements (Example 2)

h	$\mathbf{e}_0(u)$	$\mathbf{r}_0(u)$	$\mathbf{e}_1(u)$	$\mathbf{r}_1(u)$	$\mathbf{e}(u)$	$\mathbf{r}(u)$
0.5190E + 0	0.2715E + 0	—	0.6502E + 0	—	0.7946E + 0	—
0.2595E + 0	0.7662E − 1	1.8251	0.3029E + 0	1.1020	0.3125E + 0	1.3463
0.1297E + 0	0.1826E − 1	2.0678	0.1109E + 0	1.4487	0.1124E + 0	1.4743
0.6488E − 1	0.4417E − 2	2.0489	0.4202E − 1	1.4365	0.4225E − 1	1.4125
0.3244E − 1	0.1089E − 2	2.0201	0.1785E − 1	1.2351	0.1789E − 1	1.2398
0.1622E − 1	0.2709E − 3	2.0072	0.8334E − 2	1.0988	0.8338E − 2	1.1013
0.8110E − 2	0.6876E − 4	1.9781	0.4069E − 2	1.0343	0.4070E − 2	1.0346
h	$\mathbf{e}(\boldsymbol{\sigma})$	$\mathbf{r}(\boldsymbol{\sigma})$	$\mathbf{e}(\xi)$	$\mathbf{r}(\xi)$	$\mathbf{e}$	$\mathbf{r}(\mathbf{e})$
0.5190E + 0	0.1520E + 1	—	0.8945E + 0	—	0.1899E + 1	—
0.2595E + 0	0.7674E + 0	0.9860	0.4095E + 0	1.1272	0.9243E + 0	1.0388
0.1297E + 0	0.3583E + 0	1.0982	0.1504E + 0	1.4442	0.4045E + 0	1.1915
0.6488E − 1	0.1724E + 0	1.0561	0.5657E − 1	1.4116	0.1863E + 0	1.1193
0.3244E − 1	0.8503E − 1	1.0197	0.2290E − 1	1.3046	0.8986E − 1	1.0519
0.1622E − 1	0.4232E − 1	1.0066	0.1009E − 1	1.1824	0.4430E − 1	1.0203
0.8110E − 2	0.2135E − 1	0.9871	0.4811E − 2	1.0685	0.2205E − 1	1.0065

Table 3
Individual errors, total errors, and experimental rates of convergence for a sequence of uniform refinements (Example 3)

h	$\mathbf{e}_0(u)$	$\mathbf{r}_0(u)$	$\mathbf{e}_1(u)$	$\mathbf{r}_1(u)$	$\mathbf{e}(u)$	$\mathbf{r}(u)$
0.5190E + 0	0.5994E − 1	—	0.1489E + 0	—	0.1606E + 0	—
0.2595E + 0	0.1244E − 1	2.2685	0.4699E − 1	1.6639	0.4861E − 1	1.7241
0.1297E + 0	0.2956E − 2	2.0721	0.1579E − 1	1.5724	0.1606E − 1	1.5968
0.6488E − 1	0.7229E − 3	2.0331	0.6021E − 2	1.3918	0.6064E − 2	1.4060
0.3244E − 1	0.1793E − 3	2.0114	0.2650E − 2	1.1840	0.2656E − 2	1.1910
0.1622E − 1	0.4472E − 4	2.0033	0.1266E − 2	1.0657	0.1266E − 2	1.0689
0.8110E − 2	0.8827E − 5	2.3409	0.6237E − 3	1.0213	0.6238E − 3	1.0211
h	$\mathbf{e}(\boldsymbol{\sigma})$	$\mathbf{r}(\boldsymbol{\sigma})$	$\mathbf{e}(\xi)$	$\mathbf{r}(\xi)$	$\mathbf{e}$	$\mathbf{r}(\mathbf{e})$
0.5190E + 0	0.1609E + 0	—	0.1751E + 0	—	0.2869E + 0	—
0.2595E + 0	0.5859E − 1	1.4574	0.6883E − 1	1.3470	0.1026E + 0	1.4835
0.1297E + 0	0.1881E − 1	1.6382	0.2188E − 1	1.6525	0.3302E − 1	1.6347
0.6488E − 1	0.7023E − 2	1.4222	0.7924E − 2	1.4662	0.1220E − 1	1.4374
0.3244E − 1	0.3062E − 2	1.1976	0.3285E − 2	1.2703	0.5218E − 2	1.2253
0.1622E − 1	0.1459E − 2	1.0694	0.1484E − 2	1.1464	0.2436E − 2	1.0989
0.8110E − 2	0.7186E − 3	1.0217	0.7162E − 3	1.0510	0.1191E − 2	1.0323

Theorem 3.2 (when $r = 1$) is attained in all the examples, which confirms the a priori error estimate provided by that theorem. Moreover, we also notice a quadratic order of convergence for the error $\mathbf{e}_0(u)$, whose theoretical proof follows from usual duality arguments.

We now show the performance of the associated adaptive algorithms using the a posteriori error estimates $\boldsymbol{\eta}$ and $\boldsymbol{\theta}$. In this case, the experimental rate of convergence $\mathbf{r}(\mathbf{e})$ is defined by $\mathbf{r}(\mathbf{e}) := -2\log(\mathbf{e}/\mathbf{e}')/\log(N/N')$, where $\mathbf{e}$ and $\mathbf{e}'$ denote the total errors at two consecutive triangulations with N and N' degrees of freedom, respectively. In addition, the mesh refinement process follows a standard approach from [25], which considers a parameter $\gamma \in (0, 1)$ and reads as follows:

1. Start with a coarse mesh $\mathscr{T}_h$.
2. Solve the discrete problem (3.5) for the actual mesh $\mathscr{T}_h$.
3. Compute η_T (θ_T) for each triangle $T \in \mathscr{T}_h$.

Table 4
Individual errors, total errors, experimental rates of convergence, a posteriori error estimates, and effectivity indices for the uniform refinement (Example 4)

N	$\mathbf{e}(u)$	$\mathbf{e}(\boldsymbol{\sigma})$	$\mathbf{e}(\xi)$	$\mathbf{e}$	$\mathbf{r}(\mathbf{e})$	$\boldsymbol{\eta}$	$\mathbf{e}/\boldsymbol{\eta}$	$\boldsymbol{\theta}$	$\mathbf{e}/\boldsymbol{\theta}$
33	0.86E + 2	0.14E + 3	0.11E + 2	0.20E + 3	—	0.17E + 3	1.182	0.15E + 3	1.282
123	0.94E + 2	0.12E + 4	0.11E + 3	0.12E + 4	—	0.12E + 4	1.007	0.12E + 4	1.008
471	0.26E + 2	0.11E + 4	0.45E + 2	0.11E + 4	0.171	0.11E + 4	0.998	0.10E + 4	1.000
1839	0.19E + 2	0.51E + 3	0.26E + 2	0.51E + 3	1.097	0.51E + 3	0.992	0.51E + 3	0.999
7263	0.93E + 1	0.24E + 3	0.14E + 2	0.24E + 3	1.069	0.25E + 3	0.990	0.25E + 3	0.999
28 863	0.45E + 1	0.12E + 3	0.68E + 1	0.12E + 3	0.999	0.12E + 3	0.991	0.12E + 3	1.000
115 071	0.22E + 1	0.61E + 2	0.32E + 1	0.61E + 2	1.001	0.62E + 2	0.992	0.61E + 2	1.001

Table 5
Individual errors, total errors, experimental rates of convergence, a posteriori error estimates, and effectivity indices for the corresponding adaptive refinements (Example 4)

N	$\mathbf{e}(u)$	$\mathbf{e}(\boldsymbol{\sigma})$	$\mathbf{e}(\xi)$	$\mathbf{e}$	$\mathbf{r}(\mathbf{e})$	$\boldsymbol{\eta}$	$\mathbf{e}/\boldsymbol{\eta}$
33	0.862E + 2	0.139E + 3	0.107E + 3	0.195E + 3	—	0.165E + 3	1.1824
53	0.114E + 3	0.120E + 4	0.127E + 3	0.121E + 4	—	0.120E + 4	1.0115
79	0.251E + 2	0.107E + 4	0.436E + 2	0.108E + 4	0.5968	0.108E + 4	0.9976
107	0.235E + 2	0.512E + 3	0.447E + 2	0.514E + 3	4.8641	0.519E + 3	0.9901
133	0.221E + 2	0.267E + 3	0.390E + 2	0.271E + 3	5.8820	0.279E + 3	0.9703
297	0.133E + 2	0.145E + 3	0.222E + 2	0.147E + 3	1.5169	0.151E + 3	0.9741
746	0.987E + 1	0.804E + 2	0.163E + 2	0.826E + 2	1.2576	0.873E + 2	0.9461
1102	0.758E + 1	0.693E + 2	0.114E + 2	0.707E + 2	0.8003	0.734E + 2	0.9623
2731	0.486E + 1	0.399E + 2	0.770E + 1	0.409E + 2	1.2016	0.431E + 2	0.9494
4691	0.326E + 1	0.335E + 2	0.468E + 1	0.340E + 2	0.6863	0.353E + 2	0.9631
10 592	0.250E + 1	0.203E + 2	0.348E + 1	0.207E + 2	1.2152	0.219E + 2	0.9471
19 711	0.166E + 1	0.162E + 2	0.226E + 1	0.165E + 2	0.7423	0.172E + 2	0.9562
42 671	0.125E + 1	0.101E + 2	0.161E + 1	0.104E + 2	1.2029	0.110E + 2	0.9406

N	$\mathbf{e}(u)$	$\mathbf{e}(\boldsymbol{\sigma})$	$\mathbf{e}(\xi)$	$\mathbf{e}$	$\mathbf{r}(\mathbf{e})$	$\boldsymbol{\theta}$	$\mathbf{e}/\boldsymbol{\theta}$
33	0.862E + 2	0.139E + 3	0.107E + 2	0.195E + 3	—	0.152E + 3	1.2821
53	0.114E + 3	0.120E + 4	0.127E + 3	0.121E + 4	—	0.119E + 4	1.0125
79	0.251E + 2	0.107E + 4	0.436E + 2	0.108E + 4	0.5968	0.107E + 4	0.9999
107	0.235E + 2	0.512E + 3	0.447E + 2	0.514E + 3	4.8641	0.514E + 3	0.9988
133	0.221E + 2	0.267E + 3	0.390E + 2	0.271E + 3	5.8820	0.273E + 3	0.9921
297	0.133E + 2	0.145E + 3	0.222E + 2	0.147E + 3	1.5169	0.147E + 3	0.9978
649	0.124E + 2	0.845E + 2	0.209E + 2	0.879E + 2	1.3217	0.895E + 2	0.9812
1140	0.775E + 1	0.671E + 2	0.112E + 2	0.685E + 2	0.8875	0.685E + 2	0.9995
2605	0.551E + 1	0.403E + 2	0.864E + 1	0.416E + 2	1.2092	0.414E + 2	1.0016
4939	0.384E + 1	0.310E + 2	0.566E + 1	0.317E + 2	0.8419	0.317E + 2	0.9986
10 486	0.279E + 1	0.201E + 2	0.379E + 1	0.207E + 2	1.1393	0.205E + 2	1.0045
19 592	0.194E + 1	0.156E + 2	0.255E + 1	0.160E + 2	0.8294	0.158E + 2	1.0044
40 545	0.144E + 1	0.103E + 2	0.185E + 1	0.105E + 2	1.1444	0.104E + 2	1.0066

4. Evaluate stopping criterion and decide to finish or go to next step.
5. Use *blue-green* procedure to refine each $T' \in \mathscr{T}_h$ whose indicator $\eta_{T'}$ $(\theta_{T'})$ is greater than or equal to γ times the maximum value of the indicators η_T (θ_T), $T \in \mathscr{T}_h$.
6. Define resulting mesh as actual mesh $\mathscr{T}_h$ and go to step 2.

The examples to be considered for the adaptive algorithms are described as follows. In Example 4 we take $\Omega :=]0,1[^2$, with $\Gamma_{\mathrm{D}} := [0,1] \times \{0\} \cup \{0\} \times [0,1]$ and $\Gamma_{\mathrm{N}} := \Gamma - \bar{\Gamma}_{\mathrm{D}}$, and choose the data f and g so that the exact

Table 6
Individual errors, total errors, experimental rates of convergence, a posteriori error estimates, and effectivity indices for the uniform refinement (Example 5)

N	$\mathbf{e}(u)$	$\mathbf{e}(\boldsymbol{\sigma})$	$\mathbf{e}(\xi)$	$\mathbf{e}$	$\mathbf{r}(\mathbf{e})$	$\boldsymbol{\eta}$	$\mathbf{e}/\boldsymbol{\eta}$	$\boldsymbol{\theta}$	$\mathbf{e}/\boldsymbol{\theta}$
65	0.30E + 0	0.28E + 0	0.36E + 0	0.55E + 0	—	0.94E + 0	0.585	0.49E + 0	1.123
227	0.18E + 0	0.18E + 0	0.21E + 0	0.34E + 0	0.767	0.66E + 0	0.519	0.28E + 0	1.196
839	0.12E + 0	0.11E + 0	0.13E + 0	0.21E + 0	0.703	0.43E + 0	0.498	0.17E + 0	1.207
3215	0.77E − 1	0.76E − 1	0.83E − 1	0.13E + 0	0.683	0.28E + 0	0.487	0.11E + 0	1.205
12 575	0.49E − 1	0.48E − 1	0.51E − 1	0.86E − 1	0.675	0.18E + 0	0.481	0.71E − 1	1.202
49 727	0.31E − 1	0.30E − 1	0.32E − 1	0.54E − 1	0.671	0.11E + 0	0.477	0.45E − 1	1.199

Table 7
Individual errors, total errors, experimental rates of convergence, a posteriori error estimates, and effectivity indices for the corresponding adaptive refinements (Example 5)

N	$\mathbf{e}(u)$	$\mathbf{e}(\boldsymbol{\sigma})$	$\mathbf{e}(\xi)$	$\mathbf{e}$	$\mathbf{r}(\mathbf{e})$	$\boldsymbol{\eta}$	$\mathbf{e}/\boldsymbol{\eta}$
65	0.305E + 0	0.288E + 0	0.360E + 0	0.554E + 0	—	0.947E + 0	0.5845
196	0.194E + 0	0.188E + 0	0.232E + 0	0.357E + 0	0.7962	0.662E + 0	0.5385
292	0.141E + 0	0.138E + 0	0.171E + 0	0.261E + 0	1.5618	0.487E + 0	0.5364
407	0.112E + 0	0.110E + 0	0.138E + 0	0.209E + 0	1.3353	0.391E + 0	0.5354
821	0.745E − 1	0.751E − 1	0.894E − 1	0.138E + 0	1.1795	0.275E + 0	0.5038
1117	0.619E − 1	0.624E − 1	0.744E − 1	0.115E + 0	1.1965	0.226E + 0	0.5091
1740	0.482E − 1	0.478E − 1	0.558E − 1	0.879E − 1	1.2158	0.178E + 0	0.4924
3066	0.350E − 1	0.353E − 1	0.408E − 1	0.643E − 1	1.1052	0.133E + 0	0.4821
4569	0.280E − 1	0.280E − 1	0.317E − 1	0.508E − 1	1.1816	0.107E + 0	0.4713
7347	0.221E − 1	0.220E − 1	0.250E − 1	0.400E − 1	1.0025	0.853E − 1	0.4692
11 772	0.171E − 1	0.171E − 1	0.193E − 1	0.310E − 1	1.0877	0.669E − 1	0.4630
18 062	0.138E − 1	0.137E − 1	0.152E − 1	0.247E − 1	1.0519	0.542E − 1	0.4566
29 069	0.110E − 1	0.108E − 1	0.121E − 1	0.196E − 1	0.9655	0.430E − 1	0.4570

N	$\mathbf{e}(u)$	$\mathbf{e}(\boldsymbol{\sigma})$	$\mathbf{e}(\xi)$	$\mathbf{e}$	$\mathbf{r}(\mathbf{e})$	$\boldsymbol{\theta}$	$\mathbf{e}/\boldsymbol{\theta}$
65	0.305E + 0	0.288E + 0	0.3609E + 0	0.554E + 0	—	0.493E + 0	1.1232
218	0.190E + 0	0.186E + 0	0.2222E + 0	0.346E + 0	0.7733	0.289E + 0	1.1998
278	0.140E + 0	0.138E + 0	0.1635E + 0	0.256E + 0	2.4982	0.219E + 0	1.1648
443	0.105E + 0	0.103E + 0	0.1204E + 0	0.190E + 0	1.2667	0.168E + 0	1.1322
721	0.852E − 1	0.834E − 1	0.9541E − 1	0.152E + 0	0.9098	0.126E + 0	1.2032
1227	0.591E − 1	0.586E − 1	0.6717E − 1	0.107E + 0	1.3392	0.907E − 1	1.1790
1512	0.521E − 1	0.520E − 1	0.5788E − 1	0.937E − 1	1.2689	0.787E − 1	1.1894
2571	0.389E − 1	0.391E − 1	0.4266E − 1	0.697E − 1	1.1118	0.574E − 1	1.2146
3660	0.317E − 1	0.317E − 1	0.3481E − 1	0.568E − 1	1.1607	0.468E − 1	1.2129
5707	0.249E − 1	0.250E − 1	0.2683E − 1	0.443E − 1	1.1171	0.366E − 1	1.2099
8721	0.201E − 1	0.201E − 1	0.2159E − 1	0.357E − 1	1.0180	0.291E − 1	1.2258
13 312	0.160E − 1	0.162E − 1	0.1722E − 1	0.286E − 1	1.0522	0.233E − 1	1.2251
21 517	0.125E − 1	0.126E − 1	0.1329E − 1	0.222E − 1	1.0527	0.181E − 1	1.2249
32 613	0.101E − 1	0.102E − 1	0.1069E − 1	0.179E − 1	1.0289	0.145E − 1	1.2295

solution is

$$u(\mathbf{x}) := \frac{x_1 x_2}{(x_1 - 1)^2 + (x_2 - 1)^2 + 0.01} \quad \forall \mathbf{x} := (x_1, x_2) \in \Omega.$$

We observe that u vanishes at Γ_{D} and has a boundary layer around the point (1, 1).

Next, in Example 5 we consider the L-shaped domain $\Omega :=]-1, 1[^2 - [0, 1]^2$, with $\Gamma_{\mathrm{D}} := [0, 1] \times \{0\} \cup \{0\} \times [0, 1]$ and $\Gamma_{\mathrm{N}} := \Gamma - \bar{\Gamma}_{\mathrm{D}}$, and chose the data f and g so that the exact solution, in polar coordinates (r, ϑ), is given by

$$u(r, \vartheta) := r^{2/3} \sin\left(\frac{2\vartheta - \pi}{3}\right) \quad \forall (r, \vartheta) \in \Omega.$$

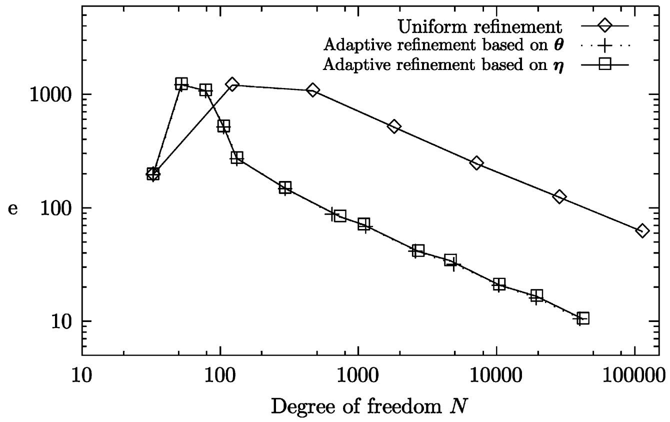

Fig. 1. **e** vs. N for the uniform and adaptive refinements (Example 4).

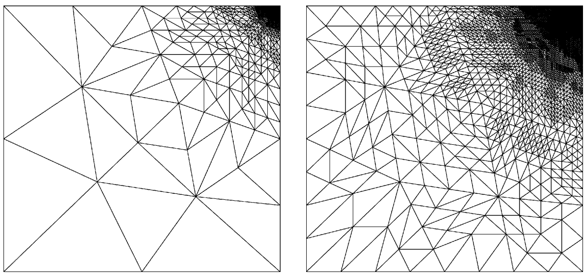

Fig. 2. Adapted intermediate meshes with 2731 and 42 671 degrees of freedom for the adaptive refinement based on $\boldsymbol{\eta}$ (Example 4).

It is easy to see that u vanishes at Γ_{D}, which holds for $\vartheta = \pi/2$ and $\vartheta = 2\pi$. In addition, because of the power of r, the partial derivatives of u are singular at the origin. According to this singularity, Theorem 3.2 yields a rate of convergence of $\mathrm{O}(h^{2/3})$ for the augmented mixed finite element scheme (3.5).

In Tables 4–7, we provide the errors for each unknown, the total error, the experimental rates of convergence, the a posteriori error estimates $\boldsymbol{\eta}$ and $\boldsymbol{\theta}$, and the corresponding effectivity indices $\mathbf{e}/\boldsymbol{\eta}$ and $\mathbf{e}/\boldsymbol{\theta}$ for the uniform and adaptive refinements. We use $\gamma = 0.5$ and 0.3 for Examples 4 and 5, respectively. We observe here that the indices $\mathbf{e}/\boldsymbol{\eta}$ and $\mathbf{e}/\boldsymbol{\theta}$ remain always bounded above and below, which confirms the reliability of $\boldsymbol{\eta}$ and $\boldsymbol{\theta}$, and the efficiency of $\boldsymbol{\eta}$. Moreover, this fact provides also numerical evidences for the eventual efficiency of $\boldsymbol{\theta}$. Next, Figs. 1 and 4 show **e** vs. the degrees of freedom N. As expected, the total error **e** of each adaptive algorithm decreases much faster than that of the uniform one. This property is particularly notorious in Example 5 where the experimental rates of convergence of the adaptive algorithms (see Table 7) recover the quasi-optimal order h, thus improving the rate $\frac{2}{3}$ obtained with the uniform refinement (see Table 6). Finally, Figs. 2, 3, 5, and 6 display some intermediate meshes obtained with the adaptive refinements. It is important to verify that both algorithms are able to recognize the singularities of the solution u. In particular, this is observed in Example 4 (cf. Figs. 2 and 3) where the adapted meshes are highly refined around (1, 1). Similarly, the adapted meshes obtained in Example 5 (cf. Figs. 5 and 6) concentrate the corresponding refinements around the origin. In addition, we notice in Example 5 (see Fig. 6) that the adaptive algorithm based on $\boldsymbol{\theta}$ also tends to slightly refine in a neighborhood of the Neumann boundary, which should be explained by the terms $\kappa(T)\|\boldsymbol{\sigma}_h - \nabla\bar{u}_h\|^2_{[L^2(T)]^2}$ and $\kappa(T)\|u_h - \bar{u}_h\|^2_{L^2(T)}$ appearing in the definition of the local indicator θ_T (cf. (5.19)). However, this effect is not observed explicitly in Example 4 (see Fig. 3) since the point (1, 1) (around which the boundary layer holds) lies precisely on the Neumann boundary of the problem.

Summarizing, the numerical results presented in this section constitute enough support for the adaptive algorithms being much more efficient than a uniform discretization when solving our augmented mixed finite element scheme.

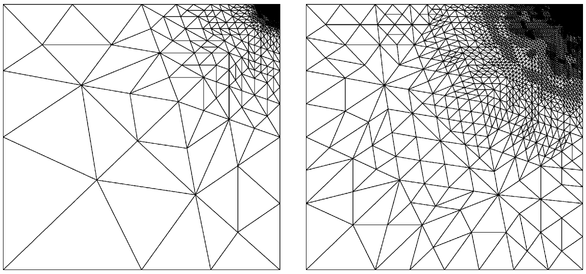

Fig. 3. Adapted intermediate meshes with 2605 and 40 545 degrees of freedom for the adaptive refinement based on $\boldsymbol{\theta}$ (Example 4).

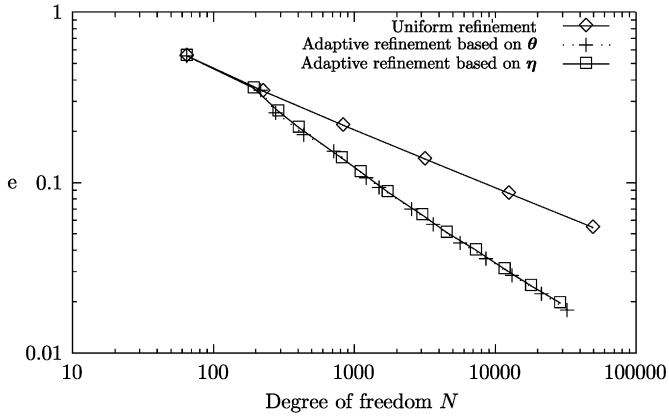

Fig. 4. **e** vs. N for the uniform and adaptive refinements (Example 5).

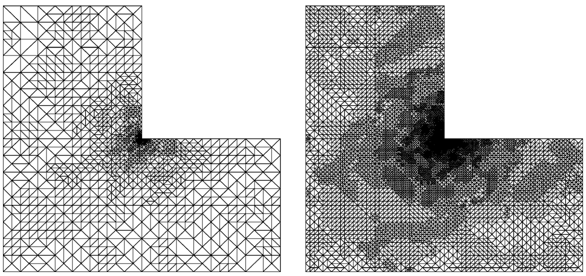

Fig. 5. Adapted intermediate meshes with 4569 and 29 069 degrees of freedom for the adaptive refinement based on $\boldsymbol{\eta}$ (Example 5).

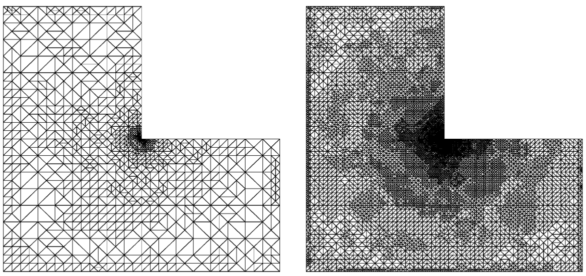

Fig. 6. Adapted intermediate meshes with 3660 and 32 613 degrees of freedom for the adaptive refinement based on $\boldsymbol{\theta}$ (Example 5).

References

[1] I. Babuška, A.K. Aziz, Survey lectures on the mathematical foundations of the finite element method, in: A.K.Aziz(ed.) (Ed.), The Mathematical Foundations of the Finite Element Method with Applications to Partial Differential Equations, Academic Press, New York, 1972.
[2] I. Babuška, G.N. Gatica, On the mixed finite element method with Lagrange multipliers, Numer. Methods Partial Differential Equations 19 (2) (2003) 192–210.
[3] M.A. Barrientos, G.N. Gatica, E.P. Stephan, A mixed finite element method for nonlinear elasticity: two-fold saddle point approach and a posteriori error estimate, Numer. Math. 91 (2) (2002) 197–222.
[4] T.P. Barrios, G.N. Gatica, F. Paiva, A wavelet-based stabilization of the mixed finite element method with Lagrange multipliers, Appl. Math. Lett. 19 (3) (2006) 244–250.
[5] F. Brezzi, M. Fortin, Mixed and Hybrid Finite Element Methods, Springer, New York, NY, 1991.
[6] F. Brezzi, M. Fortin, A minimal stabilisation procedure for mixed finite element methods, Numer. Math. 89 (3) (2001) 457–491.
[7] F. Brezzi, M. Fortin, L.D. Marini, Mixed finite element methods with continuous stresses, Math. Models Methods Appl. Sci. 3 (2) (1993) 275–287.
[8] R. Bustinza, G.N. Gatica, M. González, S. Meddahi, E.P. Stephan, Enriched finite element subspaces for dual-dual mixed formulations in fluid mechanics and elasticity, Comput. Methods Appl. Mech. Eng. 194 (2–5) (2005) 427–439.
[9] C. Carstensen, An a posteriori error estimate for a first-kind integral equation, Math. Comput. 66 (217) (1997) 139–155.
[10] C. Carstensen, A posteriori error estimate for the mixed finite element method, Math. Comput. 66 (218) (1997) 465–476.
[11] P.G. Ciarlet, The Finite Element Method for Elliptic Problems, North-Holland, Amsterdam, 1978.
[12] P. Clément, Approximation by finite element functions using local regularisation, RAIRO, Analise Numérique 9 (1975) 77–84.
[13] J. Douglas, J. Wan, An absolutely stabilized finite element method for the Stokes problem, Math. Comput. 52 (186) (1989) 495–508.
[14] L.P. Franca, New mixed finite element methods, Ph.D. Thesis, Stanford University, 1987.
[15] L.P. Franca, T.J.R. Hughes, Two classes of finite element methods, Comput. Methods Appl. Mech. Eng. 69 (1988) 89–129.
[16] L.P. Franca, R. Stenberg, Error analysis of Galerkin least squares methods for the elasticity equations, SIAM J. Numer. Anal. 28 (6) (1991) 1680–1697.
[17] G.N. Gatica, A note on the efficiency of residual-based a posteriori error estimators for some mixed finite element methods, Electron. Trans. Numer. Anal. 17 (2004) 218–233.
[18] G.N. Gatica, Analysis of a new augmented mixed finite element method for linear elasticity allowing $\mathbb{R}T_0$-$\mathbb{P}_1$-$\mathbb{P}_0$ approximations, Math. Modelling Numer. Anal. 40(1), to appear.
[19] G.N. Gatica, M. Maischak, A-posteriori error estimates for the mixed finite element method with Lagrange multipliers, Numer. Methods Partial Differential Equations 21 (3) (2005) 421–450.
[20] V. Girault, P.-A. Raviart, Finite Element Methods for Navier–Stokes Equations, Theory and Algorithms, Springer, Berlin, 1986.
[21] A. Masud, T.J.R. Hughes, A stabilized mixed finite element method for Darcy flow, Comput. Methods Appl. Mech. Eng. 191 (2002) 4341–4370.
[22] J.E. Roberts, J.-M. Thomas, Mixed and hybrid methods, in: P.G. Ciarlet, J.L. Lions (Eds.), Handbook of Numerical Analysis, vol. II, Finite Element Methods (Part 1), 1991, North-Holland, Amsterdam.
[23] A. Stroud, Approximate Calculation of Multiple Integrals, Prentice-Hall, Englewood Cliffs, 1971.
[24] R. Verfürth, A posteriori error estimation and adaptive mesh-refinement techniques, J. Comput. Appl. Math. 50 (1994) 67–83.
[25] R. Verfürth, A Review of a Posteriori Error Estimation and Adaptive Mesh-Refinement Techniques, Wiley-Teubner, Chichester, 1996.